CHALMERS
UNIVERSITY OF TECHNOLOGY

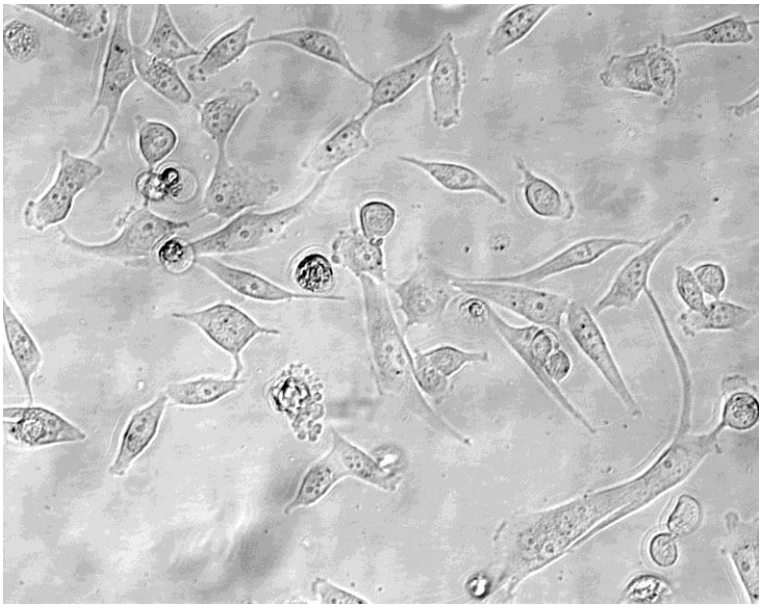

Structural analysis of β-arrestin signalling at Protease-activated receptor 2 (PAR2)

Evaluation of amino acids E232, Y323, Y326, Y82 and D228 of PAR2 for agonists SLIGKV, SLIGRL, 2f-LIGRLO and GB110 in β-arrestin-mediated signalling

Master's thesis within the Biotechnology Master Program

JONATHAN JOGENSJÖ

Department of Biology and Biological Engineering
CHALMERS UNIVERSITY OF TECHNOLOGY
Gothenburg, Sweden 2018

MASTER'S THESIS 2018

Structural analysis of β-arrestin signalling at Protease-activated receptor 2 (PAR2)

Evaluation of amino acids E232, Y323, Y326, Y82 and D228 of PAR2 for agonists SLIGKV, SLIGRL, 2f-LIGRLO and GB110 in β-arrestin-mediated signalling

Jonathan Jogensjö

CHALMERS
UNIVERSITY OF TECHNOLOGY

Department of Biology and Biological Engineering
CHALMERS UNIVERSITY OF TECHNOLOGY
Mechanistic Biology and Profiling, Discovery Sciences,
IMED Biotech unit, AstraZeneca, Gothenburg
Gothenburg, Sweden 2018

Structural analysis of β-arrestin signalling at Protease-activated receptor 2 (PAR2)
Evaluation of amino acids E232, Y323, Y326, Y82 and D228 of PAR2 for agonists SLIGKV, SLIGRL, 2f-LIGRLO and GB110 in β-arrestin-mediated signalling
JONATHAN JOGENSJÖ

Supervisor: Amanda Kennedy
Mechanistic Biology and Profiling
Discovery Sciences
IMED Biotech unit
AstraZeneca, Gothenburg

Examiner: Dina Petranovic Nielsen
Department of Biology and Biological Engineering
Division of Systems and Synthetic Biology
Chalmers University of Technology

Master's Thesis 2018
Mechanistic Biology and Profiling
AstraZeneca, Gothenburg

Cover: Transiently transfected 1321N1 β-arrestin-EA cells with PAR2 (V5)-PK Wild-Type.

Gothenburg, Sweden 2018

JONATHAN JOGENSJÖ
Chalmers University of Technology

Abstract

G protein-coupled receptors (GPCRs) are the most common receptor class for drug targeting. They are key targets for more than 35% of clinically used drugs as they are important in controlling a diversity of processes within pathophysiology. GPCR signalling was first thought to only be G protein-mediated. However, it has recently been shown that β-arrestins can act as an adaptor protein creating their own G protein-independent signalling. One GPCR, the protease-activated receptor 2 (PAR2), has been shown to be involved in inflammation and pain; metabolic, cardiovascular and neurological systems but also cancers which makes it an interesting drug target. Recently, the crystal structure of PAR2 together with two antagonists was solved indicating a suggested orthogonal binding site for agonists. The aim of this project was to evaluate possible important amino acid residues of PAR2 inducing β-arrestin recruitment for the agonists SLIGKV, SLIGRL, GB110 and 2f-LIGRLO. This was done by using single point mutated receptors based on the solved crystal structure using DiscoverX PathHunter β-Arrestin Assay for GPCR Cell Lines. The β-arrestin recruitment assay is based on an enzyme fragment complementation (EFC) technology where PAR2 is tagged with an Enzyme Donor (PK) and β-arrestin with an Enzyme Acceptor (EA). Optimization of the β-arrestin recruitment assay and construction of PAR2-PK plasmids needed for transient transfections of 1321N1 β-arrestin-EA cells were carried out. The optimized conditions for β-arrestin recruitment assay were found to be 4000 cells/well, 90 minutes of agonist incubation time and 60 minutes of detection time for the U2OS cell line stably expressing PAR2-PK and β-arrestin-EA. Constructed PAR-PK plasmids were shown to have the correct fragment sizes and sequences after ScaI restriction enzyme digestion and Sanger sequencing respectively. 1321N1 β-arrestin-EA cells transiently transfected with nine PAR2-PK plasmids were shown to have PAR2 expressed at the membrane surface for all constructed plasmids. Data suggests the importance of residues E232, Y323, Y326 and D228 of PAR2 for β-arrestin-mediated signalling induced by agonists SLIGKV, SLIGRL, GB110 (except E232) and 2f-LIGRLO. Data also suggest that the proposed orthogonal site in the published crystal structure is the orthogonal binding site in β-arrestin recruitment for agonist SLIGKV, SLIGRL, GB110 and 2f-LIGLRO.

Keywords: Protease-activated receptor 2, β-arrestin recruitment, mutational analysis, signalling, SLIGKV, SLIGRL, GB110, 2f-LIGRLO.

Acknowledgements

I would like to thank Amanda Kennedy, my supervisor, for providing me an opportunity to spend 9 months at AstraZeneca Gothenburg to learn about GPCR signalling, PAR2, mammalian cell culturing, high-throughput screening, drug discovery and much more. I'm very thankful for your help during the project progress.

I would also like to thank Dina Petranovic Nielsen, my examiner, who has supported me with encouraging thoughts during my time at AstraZeneca.

I would also like to thank David Öling for answering all my questions of for instance primer design, plasmid minipreps, PCR and for sequencing barcodes.

I would also like to thank Nils-Olov Hermansson for the 1321N1 virally transfected β-arrestin cell line that was kindly given to me.

I would also like to thank Niklas Larsson for the PK-plasmid that was kindly given to me.

I would also like to thank all people I have met the in labs AC3, KL3 and SC4 for your helpful thoughts and kind personalities.

I would like to thank my father Thomas, mother Maria and sister Elvira for your support during my project, for visiting me in Gothenburg and for taking care of me when returning to Örebro.

I would like to thank my wife Erika for her infinite support, love and for all the fun outside work.

Lastly and foremost, I would like to thank God who has provided me with strength, knowledge, opportunity to undertake this project and to learn a lot about science and myself.

Proverbs 3:5-6

[5]Trust in the LORD with all your heart and lean not on your own understanding;
[6] In all your ways submit to him, and he will make your paths straight.

Jonathan Jogensjö, Gothenburg, May 2018

Table of Contents

1 Introduction

As a pharmaceutical company AstraZeneca rely on the discovery of new drugs to promote health and living for different people with different needs. To do so a deep knowledge of a variety of areas such as drug targets, structural analysis and signalling are needed.

1.1 G protein-coupled receptors

G protein-coupled receptors (GPCRs) are the most common receptor class for drug targeting and are key targets for more than 35% of clinically used drugs since they are important controlling a diversity of processes within pathophysiology (Zhao et al., 2014b, Sriram and Insel, 2018). Current drugs targeting GPCRs are for instance positive inotropes or beta blockers on β-adrenergic receptors where they are used to treat heart failure (Rajagopal et al., 2010). GPCRs are also the largest family of cell surface receptors with more than 800 different GPCRs in human (Fredriksson et al., 2003). The receptors are important mediators of signals coupled to responses from the external world but also from other cells. Our senses of sight, smell and taste for example depend on them (Alberts et al., 2008).

All GPCRs have a similar structure; an extracellular region with three extracellular loops (EL1-EL3) and a N-terminus, a transmembrane region of seven α-helices and an intracellular region containing three intracellular loops (IL1-IL3), a helix (H8) and a C-terminus, see ***Figure 1*** (Venkatakrishnan et al., 2013). However, GPCRs can be classified into five main families in human (glutamate, rhodopsin, adhesion, frizzled/taste2 and secretin) forming the GRAFS classification system based on their sequence and structural similarity (Fredriksson et al., 2003).

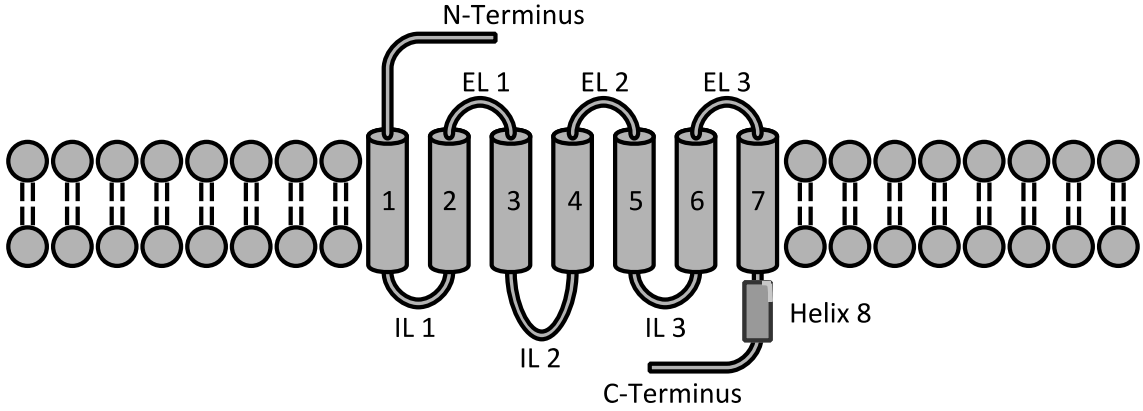

Figure 1. G protein-coupled receptor general structure with N-terminus, three extracellular loops (EL1-3), a transmembrane region of seven α-helixes (1-7), three intracellular loops (IL1-3), an intracellular helix (Helix 8) and a C-terminus.

Signal molecules binding to GPCRs are very diverse in structure and function including proteins, small peptides, hormones, neurotransmitters and photons. The same molecule can activate more than one GPCR; adrenaline for instance activates at least 9 different GPCRs (Alberts et al., 2008). Molecules changing the activity of GPCRs are agonists or antagonists; a full agonist gives a maximum response of the receptor while an antagonist results in no change of response compared to the unbound receptor and blocks the effect of an agonist. There are also partial agonists that result in a submaximal efficacy compared to a full agonist and inverse agonists that decrease the efficacy of a receptor compared to the unbound receptor state (Rajagopal et al., 2010).

Another requirement for a GPCR is the ability of the receptor to interact with a G protein upon activation. The classical mechanism for GPCR activation involves conformational

change of the receptor when an agonist binds. This change results in activation of associated heterotrimeric G proteins (Gαβγ) and further dissociation into Gα and Gβγ due to the exchange of bound GDP to GTP of the Gα subunit. The dissociation results in production of second messengers such as cyclic AMP and calcium and therefore downstream signalling cascades (Rajagopal et al., 2010). There are different kinds of G proteins; G_s which activates adenylyl cyclase allowing it to produce cyclic AMP, G_i which inactivates adenylyl cyclase, G_q which activates the inositol phospholipid pathway resulting in calcium release and $G_{12/13}$ which activates GTPases of the *Rho family* and thus regulating the actin cytoskeleton (Alberts et al., 2008). Gβγ has also been shown to produce its own signalling by for example activating phospholipase C β (PLCβ) which is involved in the inositol phospholipid pathway (Smrcka, 2008). Termination of GPCR signalling is done by GPCR kinases (GRK) which phosphorylate the GPCR intracellularly and thus recruiting β-arrestin. The binding of β-arrestin promotes desensitization and internalization of the receptor, where it is degraded or recycled to the membrane (Scarselli and Donaldson, 2009, Rajagopal et al., 2010).

More recently it has been shown that β-arrestins not only act in GPCR desensitization and internalization but also as adaptor proteins creating their own G protein-independent signalling (Shukla et al., 2014). β-arrestin-mediated signalling can involve regulation of mitogen-activated protein kinases (MAPKs) (DeFea et al., 2000) and transcriptional regulation through nuclear factor κBα (Witherow et al., 2004). Therefore, both G proteins and β-arrestins are able to recruit and interact with molecules involved in signalling, see ***Figure 2*** (Rajagopal et al., 2010).

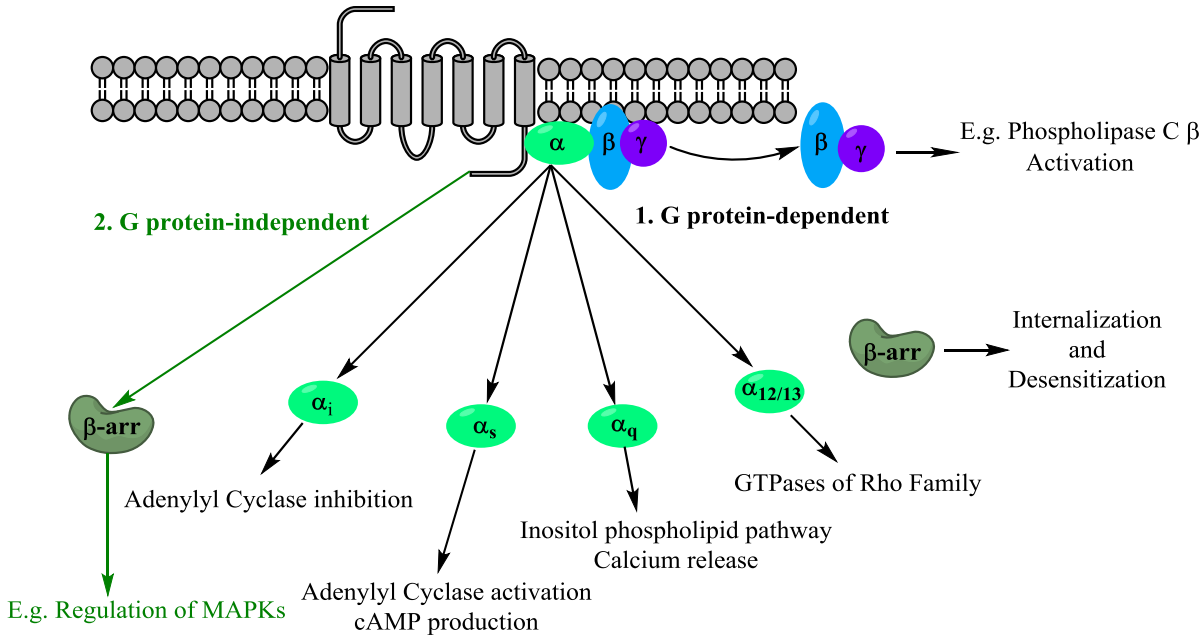

Figure 2. Activation of GPCRs leads to different signalling pathways which could be G protein-dependent (black arrows) or G protein-independent (green arrows).

1.2 Biased agonism

It was first thought that most ligands binding to GPCRs signalled equally through both G protein and β-arrestin mediated pathways. However, in some receptor-ligand arrangements one pathway is favored over another known as biased signalling (Rajagopal et al., 2010). An example of biased signalling is the 5-hydroxytrypamine (5-HT) receptor activating different G proteins when activated by different agonists (Moya et al., 2007). Another example is the study of 16 clinically relevant beta blockers of β_2-adrenergic receptor where different effects were seen in G_s and β-arrestin-mediated regulation of MAPKs (Wisler et al., 2007). One

hypothesis is that ligands alter the conformation of the receptor resulting in different signalling pathways. Biased signalling is of importance in drug design as it can selectively target a signalling pathway responsible for a physiological process or diseased state and therefore reduce side effects resulting from other pathways (Yau et al., 2013, Zhao et al., 2014b). This is an important aspect when creating drugs targeting GPCRs, such as the protease-activated receptor 2 (PAR2).

1.3 Protease-activated receptor 2 (PAR2)

Protease-activated receptor 2 (PAR2) is one of the four protease-activated receptors which are unique because they are activated through cleavage of their own extracellular N-terminus, mainly by serine proteases (Yau et al., 2013). When the N-terminus is cleaved the resulting N-terminus, a tethered ligand, self-activates the PAR by binding intramolecularly to induce signalling (Suen et al., 2017). Human PAR2, encoded by the F2RL1 gene, is mostly expressed in the gastrointestinal tract and smooth muscle but can also be found with low expression in other cell types (The Human Protein Atlas). Human PAR2 consists of 397 amino acids (see ***Appendix A*** for sequence) and can be activated by proteases such as trypsin (R^{36}/S^{37}) and cathespin-S (E^{56}/T^{57}) resulting in tethered ligands -VKGILS-NH_2 and -ASFEDVSFVT-NH_2 respectively. Elastase (S^{68}/V^{69}) probably activates PAR2 by a non-tethered ligand mechanism since its cleavage site is close to the membrane, see ***Figure 3***. The corresponding mouse PAR2 results in the tethered ligand -LRGILS-NH_2 when activated by trypsin. Other ligands are synthetic peptides mimicking the tethered ligands such as 2f-LIGRLO, H_2N-SLIGKV (later referred as SLIGKV) and H_2N-SLIGRL (later referred as SLIGRL) but also small molecules including GB110 (Zhao et al., 2014b). For structural formulas of SLIGKV, SLIGRL, GB110 and 2f-LIGRLO, see ***Appendix B***.

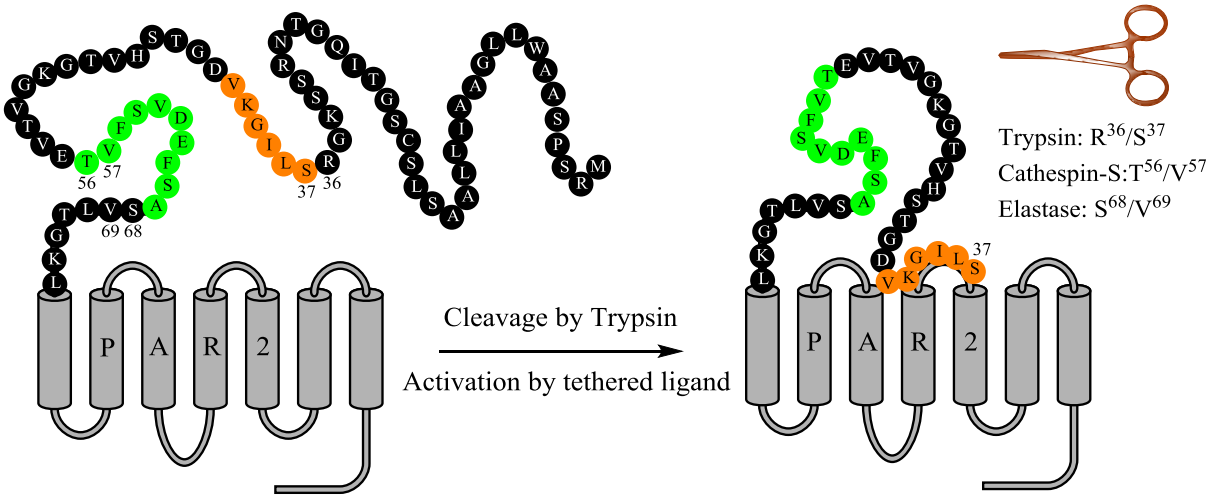

Figure 3. Protease-activated receptor 2 with N-terminus specified with amino acid sequence where cleavage sites of trypsin, cathespin-S and elastase are indicated resulting in PAR2 activation. -VKGILS-NH_2 (orange) and -ASFEDVSFVT-NH_2 (green) are tethered ligands for trypsin and cathespin-S respectively (left). Cleavage by trypsin results in tethered ligand -VKGILS-NH_2 activating PAR2 (right).

The literature suggests these agonists can induce biased signalling (Zhao et al., 2014b). For example cathespin-S has been identified as a biased agonist for PAR2-dependent inflammation and pain (Zhao et al., 2014a). Other studies have shown PAR2s involvement within metabolic (Badeanlou et al., 2011), cardiovascular (Uusitalo-Jarvinen et al., 2007) and neurological systems (Noorbakhsh et al., 2006) but also cancers (Versteeg et al., 2008) which makes it an interesting drug target. However, little is known about the mechanism of activation and bias of PAR2.

SLIGKV has been shown to induce PAR2 β-arrestin-mediated MAPK signalling in for example tumor cell migration (Ge et al., 2004) and PAR2 β-arrestin-mediated endocytosis (DeFea et al., 2000). 2f-LIGRLO has also been shown to induce PAR2 β-arrestin-mediated MAPK signalling tumor cell migration (Ge et al., 2004) but also chemotaxis (Zoudilova et al., 2010). Trypsin have been shown to induce PAR2 β-arrestin-recruitment (Ayoub and Pin, 2013) and PAR2 β-arrestin-mediated MAPK signalling (Ramachandran et al., 2011). However, more studies are needed to understand these agonists importance within PAR2 β-arrestin-mediated signalling. This could for example be evaluating amino acids of PAR2 inducing β-arrestin-mediated signalling for agonists SLIGKV, SLIGRL, 2f-LIGRLO and GB110.

Recently the crystal structures together with two distinct antagonists, AZ3451 and AZ8838, were solved giving a hint of where agonists bind to PAR2. AZ8838 binds to an allosteric pocket next to the suggested orthogonal site separated by H227 and AZ3451 to a remote allosteric site, see ***Figures 4a-c*** (Cheng et al., 2017). Further studies are needed to understand the active state of PAR2 and if its conformation varies depending on agonist and signalling pathway.

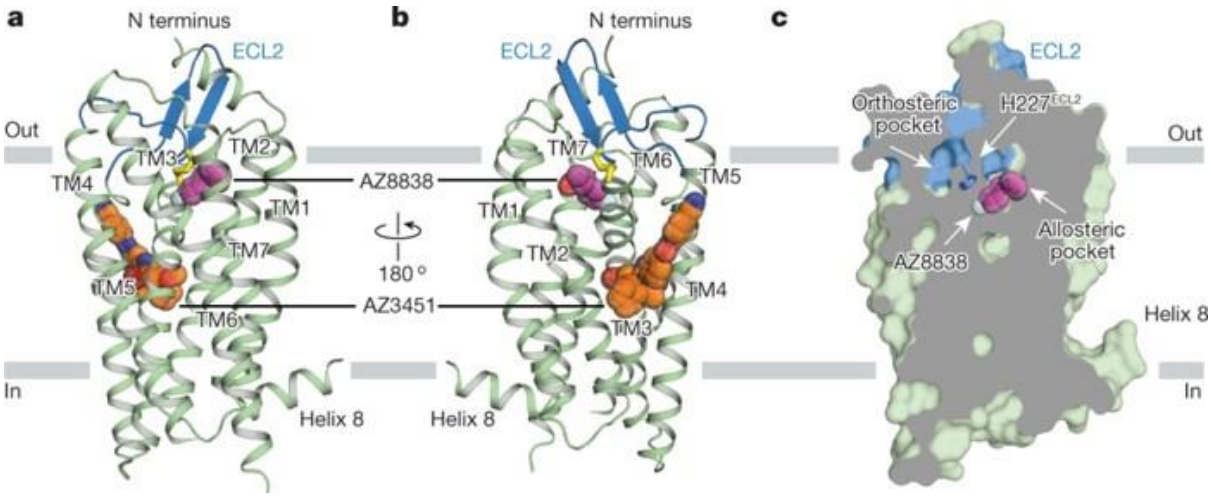

Figures 4a-c. a-b) Picture representations of PAR2 from two different angles where AZ3451(orange) binds to a remote allosteric site while AZ8838 (magenta) binds to an allosteric site close to the suggested orthogonal pocket (blue). Transmembrane domains (TM1-TM7) and extracellular loop (ECL2) are also visualized together with Helix 8 and a N-terminus. c) A surface representation of PAR2 in the same angle as a) where AZ8838 is separated from the suggested orthogonal pocket by H227 located at ECL2. Picture taken from (Cheng et al., 2017).

1.4 Aim

The aim of this study was to investigate β-arrestin signalling at PAR2 by monitoring recruitment to the receptor when activated by known agonists SLIGKV, SLIGRL, GB110 and 2f-LIGRLO. Then, to further characterize the effects of these agonists by identifying key amino acids of PAR2 necessary for β-arrestin recruitment through mutational analysis.

1.5 Limitations

A recombinant cell line which is not truly representative to the human endogenous environment is used. Due to time constraints, seven single point mutations of PAR2 were evaluated.

1.6 Specification of issue under investigation

The following hypotheses are considered in this project:

- PAR2 agonists (2f-LIGRLO, GB110 and SLIGKV and SLIGRL) result in different effects on β-arrestin recruitment.
- Agonist binding site is the suggested orthogonal binding site found in (Cheng et al., 2017).

2 Theory

2.1 β-Arrestin Assay for GPCR Cell Lines

The DiscoverX PathHunter β-Arrestin Assay for GPCR Cell Lines detects β-arrestin recruitment of GPCR cell lines using an Enzyme Fragment Complementation (EFC) technology. It uses the enzyme β-galactosidase (β-gal) which is split into two different fragments; an Enzyme Donor (ED) and Enzyme Acceptor (EA). When used independently these fragments show no β-gal activity. However, when brought together they form an active β-gal enzyme. In this case PAR2 is tagged with a ProLink™ (PK) which corresponds to the ED while β-arrestin is tagged with EA. When β-arrestin is recruited to PAR2 the PK and EA complement each other resulting in a functional β-gal enzyme. The enzyme then hydrolyzes a substrate present in the PathHunter detection reagent to generate light, see ***Figure 5*** (DiscoverX, 2017).

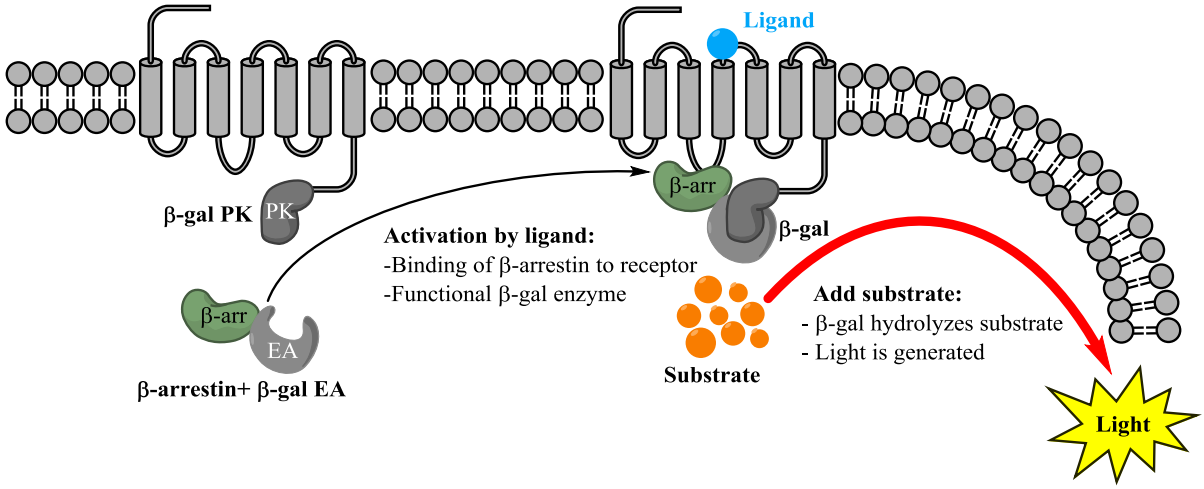

Figure 5. β-arrestin recruitment assay which upon receptor activation by ligand produces a functional β-galactosidase enzyme through β-arrestin recruitment to the PAR2. β-gal hydrolyzes added substrate and light is generated. Figure modified from (DiscoverX, 2017).

2.2 FLIPR for imaging calcium release

Fluorescence Imaging Plate Reader (FLIPR) is used for high throughput screening for cell-based fluorescent assays (Schroeder and Neagle, 1996). It could for example be used to evaluate G_q-protein-mediated signalling by looking at released Ca^{2+} from the endoplasmic reticulum to the cytosol (Zhang et al., 2003). There are different calcium kits available. One of them is the Screen Quest™ Flou-8 No wash Calcium Assay Kit which uses the fluorophore Fluo-8 that can cross cell membranes. Inside the cell a lipophilic group of Fluo-8 is cleaved by an esterase resulting in a fluorescent dye which on binding to calcium emits greater fluorescence. So, when cells are stimulated by agonists using this kit, it results in G_q-protein activation and thereby calcium release from the endoplasmic reticulum and there is enhanced fluorescence (100-250 times). This fluorescence can then be measured by FLIPR in a 384 well plate format (AAT Bioquest, 2017).

2.3 Analysis

A mathematical model is needed to describe binding of β-arrestin recruitment to the receptor or calcium release from the endoplasmic reticulum in relation to their chemiluminescent and fluorescent response respectively. For this the Hill equation can be applied to obtain concentration-response curves.

Assumptions made when obtaining the Hill equation are that the binding reaction has reached equilibrium, the free concentration of ligand doesn't significantly differ from the total ligand concentrations and only free ligand, free receptor and fully bound ligand-receptor complex forms are permitted (Gesztelyi et al., 2012, Prinz, 2010).

A concentration-response curve describes the relationship between a response and the increasing dose (or concentration) of a drug. When the concentration of a drug is increased the response changes. Usually a concentration-response curve has a wide range of concentrations. Therefore the concentration-response curve is visualized as a semi-logarithmic plot where the response (Y-axis) is linear and the concentration logarithmic (X-axis) (Golan, 2011).

Parameters such as E_{max}, E_{min}, EC_{50}, pEC_{50} and window are determined from concentration-response curves. E_{max} is the highest efficacy (response) obtained by an agonist (Neubig et al., 2003). E_{min} is described as the baseline response without agonist and the window as E_{max} subtracted by E_{min}. EC_{50} and pEC_{50} are a measure of potency which is an expression used to describe agonist activity. EC_{50} is the molar concentration of agonist which produces 50% of the maximal possible effect of that agonist whereas pEC_{50} is the negative logarithm to base 10 of an agonist's EC_{50} value (Neubig et al., 2003). pEC_{50} can be used to characterize the standard error because the concentrations are equally spaced on a log scale so pEC_{50} measures the uncertainty in both directions (GraphPad, 2017). The standard error of the mean (SEM) evaluates how precise the estimate of the mean is and can be calculated using ***Equation 1*** (Nagele, 2003).

$$\frac{\sigma}{\sqrt{n}} \qquad \textit{Equation 1}$$

Where σ is the standard deviation of the sample population and n is the sample number of observations (Nagele, 2003). A concentration-response curve showing E_{min}, E_{max}, log(EC_{50}), window and SEM bar for an efficacy value at a specific concentration is visualized in ***Figure 6***.

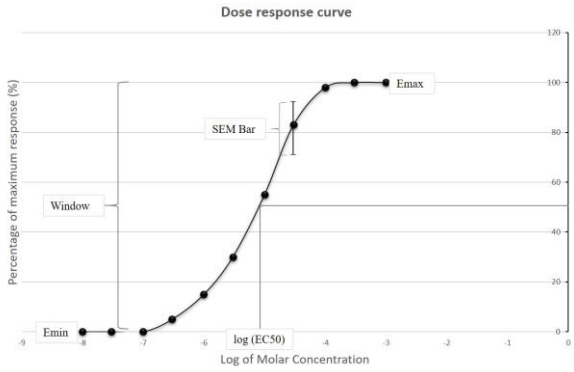

Figure 6. Concentration-response curve with E_{max}, E_{min}, log (EC_{50}), Window and SEM for an efficacy mean value visualized.

To be able to compare potencies between wild-type (WT) and different point mutations one can calculate the fold change. The fold change in this project is described according to ***Equation 2***, where the geometric mean of the EC_{50} values are used due to the concentrations are equally spaced on a logaritmic scale (GraphPad, 2018).

$$\frac{Geomean\ (\mathrm{EC_{50}\ Mut})}{Geomean\ (\mathrm{EC_{50}\ WT})} \qquad \textbf{\textit{Equation 2}}$$

GraphPad Prism 7, a software used in this project to obtain concentration-response curves, uses a four parameter logistic fit model mathematically identical to the Hill equation (Prinz, 2010, GraphPad, 2016). GraphPad software uses a nonlinear regression log(agonist) vs. response – variable slope (four parameters) mathematical model visualized in ***Equation 3*** (GraphPad, 2016).

$$Y = E_{min} + \frac{(E_{max} - E_{min})}{1 + 10^{((LogEC_{50} - X) \times n_h)}} \qquad \textbf{\textit{Equation 3}}$$

The Hill slope (n_h) describes the steepness of the curve where a Hill slope of 1 is considered as standard due to the expectation of non-cooperativity (see below). However, this model does not assume a standard slope but fits the Hill slope from the data and is therefore a variable slope model (GraphPad, 2016). The Hill slope can be used to distinguish cooperative ligand binding from non-cooperative binding. When n_h is equal to 1 there is a non-cooperative binding and thus no interaction between the different binding sites. However, if n_h is higher or lower than 1 there is positive cooperativity or negative cooperativity respectively. In positive cooperativity a binding of ligand results in a higher binding affinity in other binding sites while negative cooperativity reduces the binding affinity of binding site when a ligand has bound (Mathews et al., 2012).

2.4 U2OS and 1321N1 Cell Lines

The U2OS cell line (previously known as 2T) is a human osteosarcoma (cancerous tumor in bone) cell line which is widely used in biomedical research (Niforou et al., 2008). A commercial U2OS cell line with stable expression of PAR2-PK and β-arrestin-EA is used in this project.

The 1321N1 cell line is a human astrocytoma (brain cancer) cell line isolated in 1972 (Macintyre et al., 1972). In this project a 1321N1 cell line is used that has been virally transfected with β-arrestin-EA with Hygromycin B as selection marker. This cell line is used since it has no levels of endogenous PAR2.

2.5 Plasmids

2.5.1 PK-plasmid

The PK-plasmid, see ***Appendix D1*** for figure, contains the PK-fragment with a stop codon needed for the β-arrestin recruitment assay. Another characteristic of this plasmid is the ColE1 origin of replication allowing the plasmid to replicate in an *E.coli* host at low copy numbers (Hershfield et al., 1974). The low copy number is important when propagating plasmids containing membrane proteins (such as PAR2) as these can be toxic to the *E.coli*

host (Attrill et al., 2009). Other characteristics of this plasmid are the EMCV-IRES (the internal ribosomal entry site from encephalomyocarditis virus) allowing efficient translation in eukaryotic cells (Bochkov and Palmenberg, 2006), ampicillin and neomycin resistance genes, a FLAG tag which could be used for purification of the protein of interest and detection by antibodies (Einhauer and Jungbauer, 2001), an AAA-linker and a GGSGGGSGG-linker to be able to fuse PAR2 and the PK-tag with desired functionality (Chen et al., 2013).

2.5.2 PAR2 Plasmids

The PAR2 plasmids contain PAR2 with a CMV and T7 promoter which together works as a system to ensure high gene expression levels of PAR2 (Brisson et al., 1999). The plasmid also contains an ampicillin resistance gene with AmpR promoter, a Kozak sequence which is important for the initiation of the translation process (Kozak, 1986) and a His or V5 tag for purification and detection (Honegger et al., 1997, Tomomori-Sato et al., 2013). The difference between His and V5 PAR2 plasmids are slightly different codon optimizations used for PAR2 and a nucleotide sequence with restriction sites for PAR2 V5 prior the Kozak sequence. For plasmid map of PAR2 His plasmid, see ***Appendix D2***. Although the His/V5 tag was removed during recloning of the plasmids, throughout this report, PAR2 mutant receptors originally with a His tag were compared to PAR2 wild type with a His tag. Similarly, PAR2 mutants originally with a V5 tag were compared to PAR2 wild type V5.

2.6 Mutagenesis

In this project, a mutational analysis is performed by using single point mutations of the receptor PAR2 based on the recently solved crystal structure together with an antagonist close to the suggested orthogonal site (Cheng et al., 2017). Point mutations of PAR2 analyzed within this project and mutation descriptions are found in ***Table 1***.

Table 1. PAR2 receptors used within this project with mutation descriptions.

Receptor	Mutation descriptions
WT (V5)	No Mutation
E232A V5	Negative charge E changed to uncharged A
Y323F V5	Bulky Y changed to F (hydroxy group removed from Y)
Y326A V5	Bulky Y changed to less bulky A
Y323A V5	Bulky Y changed to less bulky A
WT (His)	No mutation
Y82F His	Bulky Y changed to F (hydroxy group removed from Y)
D228A His	Negative charge D changed to uncharged A
E232R His	Negative charge E changed to positive charge R

The amino acid residues of PAR2 to be studied (E232, Y323, Y82, D228 and Y326) are visualized in ***Figure 7***. D228 and Y82 are residues that interact with antagonist AZ8838 indicating their possible importance binding to agonists whereas E232 is localized at the extracellular loop 2 (ECL2). Residues Y323 and Y326 are also located within the suggested orthogonal binding site. Structural formulas of amino acids involved in the mutational analysis of PAR2 can be found in ***Appendix C***.

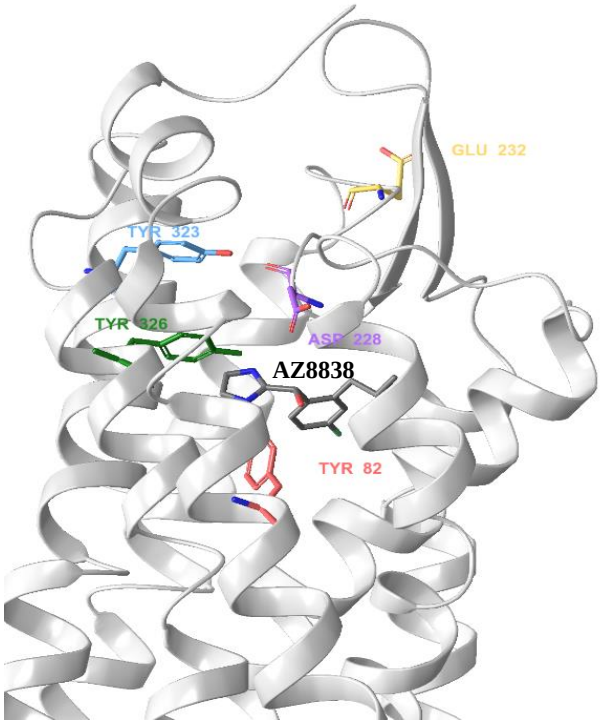

Figure 7. Structural visualization of PAR2 highlighting the amino acids E232 (yellow), Y323 (blue), Y82 (red), D228 (purple) and Y326 (green) evaluated in this project and antagonist AZ8838 (dark grey) bound in an occluded pocket. Structure adapted from the published PAR2 crystal structure (Cheng et al., 2017).

2.7 Gibson Assembly

Gibson assembly (GA) is a one-step isothermal (50°C) *in vitro* assembly method used to assemble different DNA fragments containing overlap in sequence. A 5' T5 exonuclease is used to chew on the 5'-end of double stranded DNA and thus exposing single stranded DNA. The single stranded DNA is chosen to be homologous to another formed single stranded DNA it should be annealed to. The homologous parts of the single stranded DNAs are joined together and a Phusion polymerase adds the nucleotides exonucleases chewed. Finally, a Taq ligase seals the nicks. The T5 exonuclease is labile at 50°C and is therefore inactivated during the assembly (Gibson et al., 2009), see ***Figure 8***. As the end product are plasmids there are no 5'-ends susceptible to exonuclease activity.

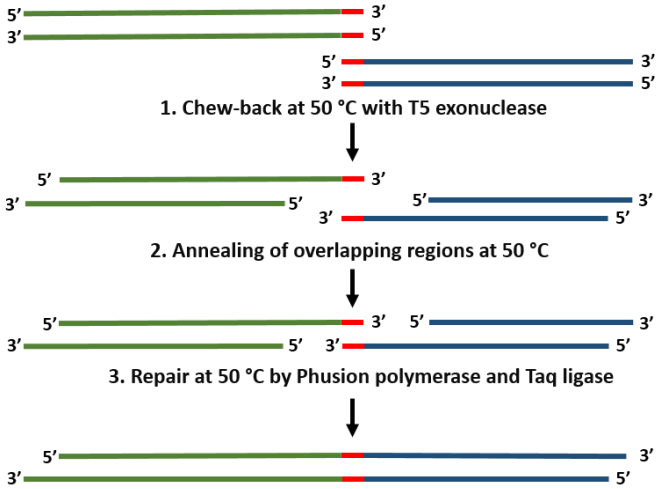

Figure 8. Gibson assembly where two fragments (green and blue) share an overlapping region (red). 1) These fragments are chewed by the T5 exonuclease, removing nucleotides from the 5'-ends. 2) This allows binding of the complementary overlapping regions. 3) Phusion polymerase adds nucleotides earlier removed and Taq ligase seals the nicks. This is all done isothermally at 50°C. The figure is modified after a picture from (Gibson et al., 2009).

2.8 MaxCyte STX® Scalable Transfection system

MaxCyte STX® Scalable Transfection system is a technology using electroporation with high cell viability and transient transfection efficiencies (MaxCyte Inc, 2017). Electroporation uses high voltage to introduce DNA into cells by increasing membrane permeability and can be used for various cell types such as mammalian cells. Mammalian cells are put in an appropriate electroporation buffer together with DNA, transferred to a cuvette and a high-voltage electrical pulse is applied allowing transfection. The cells are then allowed to recover and put in non-selective growth media (Potter and Heller, 2003).

2.9 Western Blot

Western blot is used to identify, separate and compare expression levels of proteins. Firstly, the cells containing the protein of interest(s) undergo lysis to extract the proteins. These cells are then diluted into a loading buffer followed by heating which together denature higher ordered structures but also allowing the proteins to become negatively charged. The proteins are then loaded to acrylamide gels and a voltage is applied allowing the negatively charged proteins to travel through the pores of the gel towards the positive electrode. This separates proteins by size where smaller proteins travel more rapidly compared to larger proteins. After separation, the proteins are transferred to a membrane (such as a PDVF membrane) by an electric field. The membrane is then blocked for example with 5% BSA preventing antibodies binding to the membrane unspecifically. The blocking is followed by antibody incubations and washing steps where a primary antibody binds to the protein of interest and a secondary antibody binds to the primary antibody to visualize the protein of interest (Mahmood and Yang, 2012). The secondary antibody used in this project is the Anti-Rabbit AP conjugate where the alkaline phosphatase enzyme creates a brown precepitate when adding NBT/BCIP (nitro-blue tetrazolium chloride/5-bromo-4-chloro-3’-indolyphosphate p-toluidine salt) (Leary et al., 1983).

3 Methodology

3.1 Materials

U2OS cells stably expressing PAR2-PK and β-arrestin-EA were purchased from DiscoverX and kindly propagated and cryopreserved by Amanda Kennedy (AstraZeneca, Gothenburg). The 1321N1 β-arrestin-EA cell line was kindly created and given by Nils-Olov Hermansson (AstraZeneca, Gothenburg). One Shot® TOP10 competent cells were ordered from Thermo Fisher Scientific. PAR2 plasmids were ordered from Thermo Fisher Scientific. PK-plasmid was kindly given by Niklas Larsson (AstraZeneca, Gothenburg). SLIGKV and SLIGRL were ordered from Thermo Fisher Scientific. GB110 was kindly obtained from AstraZeneca. 2f-LIGRLO was ordered from Sigma-Aldrich. All primers were ordered from Sigma-Aldrich. FastDigest ScaI restriction enzyme and corresponding buffer were ordered from Thermo Fisher Scientific. Corning#3770 microplates were ordered from Corning Life Sciences. White #781098 and #781280 microplates were ordered from Greiner Bio-One. 1.2 % E-gel with SYBR safe and E-gel 1 KB plus DNA ladder were ordered from Invitrogen. Carbenicillin plates and LB-media were obtained from AstraZeneca. NuPAGE™ sample buffer (4x), reducing buffer (10X), 4-12% Bis-Tris gels and antioxidant were ordered from Thermo Fisher Scientific. Novex Sharp Pre-stained protein standard and NBT/BCIP were ordered from Thermo Fisher Scientific. Anti-Rabbit AP (S373B) and Anti-Mouse AP (S372B) were both ordered from Promega. Anti-PAR2 (D61D5) and Anti-β-actin (A1978, AC-15) were ordered from Cell Signaling Technology and Sigma-Aldrich respectively. All cell culture reagents were ordered from Invitrogen unless other is stated.

3.2 Cell culture

3.2.1 U2OS PAR2-PK/β-arrestin-EA

The cell preparation of U2OS PAR2-PK/β-arrestin-EA cells prior assays was done by placing McCoy's 5A media with 10% FBS (in this section referred as media) in a water bath at 37 °C. 1mL of cryopreserved U2OS cells stably expressing PAR2-PK and β-arrestin-EA were then thawed in water bath at 37°C. The cells were then suspended in 10mL of preheated media prior centrifugation at 240g for four minutes. The supernatant was discarded to remove DMSO and the cell pellet was resuspended in 10mL of media. 300µL of resuspension was then counted with a Cedex HiRes analyzer using tryphan blue exclusion technology. 4000 cells in a total volume of 20µL were added to selected wells of a white 384 well plate (#781098) for β-arrestin recruitment or black 384 well plate (Corning#3770) for FLIPR using a Multidrop™ Combi Reagent Dispenser. 4000 cells were determined by β-arrestin recruitment optimization looking at different cell numbers/well (2000, 3000, 4000 and 5000). The plates were then incubated overnight in a humid incubator with 5% CO_2 at 37°C.

3.2.2 1321N1 β-arrestin-EA

1321N1 β-arrestin-EA cells were propagated by thawing cells in 37°C water bath and put in 10mL preheated DMEM GlutaMAX™ media with 10% FBS and centrifuged at 250g for 5 minutes. The supernatant was then discarded and cells resuspended with 10mL DMEM GlutaMAX™ media with 10% FBS to remove DMSO and counted in a Cedex HiRes analyzer. Cells were diluted to the desired cell density according to ***Table 2*** by a culture volume of DMEM GlutaMAX™ with 10% FBS media for one passage to allow expression of Hygromycin B resistance gene. After one passage, DMEM GlutaMAX™ with 10% FBS and 200 µg/mL Hygromycin B was used for further culturing. All culturing volumes are found in ***Table 3***.

Table 2. Cell density of 1321N1 β-arrestin-EA cells dependent on time of cultivation.

Time of Cultivation	2 days	3 days	4 days
1321N1	25000 cells/cm^2	15000 cells/cm^2	7500 cells/cm^2

When splitting cells, media was discarded from the culture vessel and cells were rinsed with calcium free PBS. Accutase® was then added to the culture vessel and incubated at 37°C for 5-10 minutes until cells had detached. DMEM GlutaMAX™ with 10% FBS and 200 µg/mL Hygromycin B (media) was added to the culture vessel and the cells were counted in a Cedex HiRes analyzer prior seeding cells according to ***Table 2***. PBS, Accutase®, media, culturing and possible rinsing media volume were added according to ***Table 3***. If needed the culturing media was exchanged with fresh media after 4-18h of cultivation.

Table 3. Volumes of PBS, Accutase®, media, media rinsing and culturing volume for culture plates/vessels 6-well plate, 25 cm^2, 225 cm^2, 1 layer, 2 layer and 5 layer.

	6 well plate	T25 25 cm^2	T225 225 cm^2	1 layer (636cm^2)	2 layer (1272 cm^2)	5 layer (3180 cm^2)
PBS	2mL	5mL	20mL	25mL	50mL	125mL
Accutase®	200µL	0.5mL	4mL	10mL	20mL	50mL
Media	1mL	4.5mL	16mL	10mL	20mL	50mL
Rinse with media	No	No	No	20mL	40mL	100mL
Culturing Volume	2mL	5mL	50mL	150mL	300mL	650mL

After transient transfection (***Section 3.8***) these cells were seeded prior assays. This was done identical as in ***Section 3.2.1*** except 1mL of 1321N1 β-arrestin-EA cells were thawed and

DMEM GlutaMAX™ media with 10% FBS was used instead of McCoy's 5A media with 10% FBS.

Residual cells after plating (200k and 1M) were collected from each transfection for use in western blot. Prior use in western blot these cells were seeded overnight in a 6-well plate (200k) or T25 prior (1M) and harvested the next day according to ***Table 3*** to ensure expression of PAR2. The cells were then collected in a 15mL Falcon tube before centrifugation at 250g for 5 minutes and removal of supernatant. The pellets were washed with 2mL PBS (200k) or 5mL PBS (1M) prior centrifugation at 250g for 5 minutes. The supernatant was then removed and the cell pellets stored at -20°C. The stored cell pellets were resuspended in 100µL ice-cold PBS followed by three freezing cycles including freezing using dry ice (5 minutes) followed by thawing at room temperature (10 minutes). The cell samples were then stored at -20°C prior use in western blot.

3.3 β-arrestin recruitment assay

Transiently transfected 1321N1 β-arrestin-EA cells with WT (V5)-PK, E232A-PK, Y323F-PK, Y326A-PK, Y323A-PK, WT (His)-PK, Y82F-PK, D228A-PK, E232R-PK and parental 1321N1 β-arrestin-EA cells (negative control) were prepared according to ***Section 3.2.2*** and evaluated in the β-arrestin recruitment assay. U2OS PAR2-PK/β-arrestin-EA cells were also evaluated as a positive control prepared as described in ***Section 3.2.1***. For all transfections and controls β-arrestin recruitment was evaluated for agonists SLIGKV (10nM-300000nM), SLIGRL (10nM-300000nM), GB110 (0.3nM-10000nM) and 2f-LIGRLO (0.3nM-10000nM).

After incubating cells overnight, a preparation plate and an agonist plate with 5X final assay concentrations (FACs) in triplicates for each agonist and each control were prepared. This was done using 384 well plate (#781280) according to calculations, see ***Appendix E*** for example.

The β-arrestin recruitment assay was then performed using the PathHunter® β-Arrestin Assay for GPCR cell lines kit following manufacturer's instruction (DiscoverX). 5µL from each well of the agonist plate was added to the corresponding cell well using Cybi-Well Vario Liquid Handler to obtain the FACs. The agonists were then incubated for 90 minutes together with the cells in a humid incubator with 5% CO_2 at 37°C. The agonist incubation time was determined to 90 minutes after optimization looking at agonist incubation times 30, 60, 90 and 120 minutes. The working detection solution was prepared with volume ratios of components found in ***Table 4*** and kept in dark.

Table 4. Working detection solution volume ratios for components cell assay buffer, substrate reagent 1 and 2.

Component	Volume ratio
Cell assay buffer	19
Substrate reagent 1	5
Substrate reagent 2	1

After incubation, 12µL of working detection solution were added to all wells containing cells with Multidrop™ Combi Reagent Dispenser. A chemiluminescent signal was then detected using EnVision™ Multilabel Plate Reader using aperture 384-LI or PHERAstar*Plus* using LUM+ optic module after 60 minutes of incubation in the dark at room temperature. The detection time was set to 60 minutes after optimization of detection time looking at 0.1, 0.5,

1, 2, 3, 4, 5, and 21 hours. FACs of SLIGKV (10nM-300000nM) was used to optimize the β-arrestin recruitment assay.

3.4 FLIPR assay

Transiently transfected 1321N1 β-arrestin-EA cells with WT (V5)-PK, E232A-PK, Y323F-PK, Y326A-PK, Y323A-PK, WT (His)-PK, Y82F-PK, D228A-PK, E232R-PK and parental 1321N1 β-arrestin-EA cells (negative control) were prepared according to ***Section 3.2.2*** and evaluated in the FLIPR assay. U2OS PAR2-PK/β-arrestin-EA cells were also evaluated as a positive control prepared as described in ***Section 3.2.1***. For all transfections and controls calcium release (FLIPR) was evaluated for agonists SLIGKV (10nM-300000nM), SLIGRL (10nM-300000nM), GB110 (0.3nM-10000nM) and 2f-LIGRLO (0.3nM-10000nM).

The same compound plate prepared in ***Section 3.3*** was used for the FLIPR assay. The FLIPR assay was performed using the Screen Quest™ Flou-8 No wash Calcium Assay Kit following manufacturer's instructions (AAT Bioquest). A 500:1 calcium dye working solution was prepared and kept in dark containing component B and Fluo-8 respectively. 20µL calcium dye was transferred to each cell well of the black Corning #3770 cell plate using a Multidrop™ Combi Reagent Dispenser. The plate was then incubated for 30 minutes with 5% CO_2 at 37°C and then in dark at room temperature for 30 minutes. 10µL from each well of the agonist plate was added to the corresponding cell well using FLIPR Tetra® High Throughput Cellular Screening System to get the FACs and fluorescence was measured.

3.5 Western blot

Transiently transfected 1321N1 β-arrestin-EA cells with WT (V5)-PK, E232A-PK, Y323F-PK, Y326A-PK, Y323A-PK, WT (His)-PK, Y82F-PK, D228A-PK, E232R-PK, parental 1321N1 β-arrestin-EA cells (negative control) were prepared according to ***Section 3.2.2*** and then evaluated in western blot together with a known 1321N1 PAR2 positive control. Expected bands for the PAR2 positive control was 32 kDa and some larger bands due to PAR2 glycosylation while the PAR2-PK fusions were expected to be larger due to the PK-tag. The expected band for β-actin was 42 kDa and was used as a loading control.

Previously collected cell lysates were used to prepare 40µl cell samples with 26µL cells, 10µL 4x NuPAGE™ sample buffer and 4µL 10x NuPAGE™ reducing buffer. The samples were then heated for 10 minutes at 70°C and 200mL 1X MES running buffer together with 500µL NuPAGE™ antioxidant were added to upper chamber. After that 600mL 1X MES running buffer was added to the lower chamber. Then 17µL of cell samples and 5µL Novex Sharp Pre-stained protein standard were loaded to two different NuPAGE™ 4-12% Bis-Tris gels (one to detect PAR2 and one to detect β-actin). The gels were then run for 35 minutes with a constant voltage of 200V. After that proteins were transferred to 0.2 µm PVDF membranes using the Trans-blot Turbo Transfer system and the Turbo 1 Mini Gel protocol (1.3A, 25V) for 7 minutes. The membranes were blocked with 1% BSA in PBS for 30 minutes with shaking. Primary antibodies, Anti-PAR2 (D61D5) and Anti-β-actin (A1978, AC-15), were then incubated 1:3000 and 1:2000 respectively with the corresponding membrane in 1% BSA with PBS for 1 hour with shaking at room temperature. The membranes were then washed with PBS and 0.05% Tween-20 three times for 5 minutes with shaking. Secondary antibodies, Anti-Rabbit AP (S373B) conjugate and Anti-Mouse AP conjugate (S372B), were then incubated 1:3000 in 1% BSA in PBS to PAR2 and β-actin membranes respectively for 1 hour with shaking at room temperature. The membranes were washed again with PBS and 0.05% Tween-20 three times for 5 minutes and a fourth time with only PBS for 5 minutes with shaking. NBT/BCIP substrate was then added to the

membranes to see alkaline phosphatase activity and thus the presence of PAR2 and β-actin. The membranes were then washed with water when the color was strong enough for visualization and comparision.

3.6 Primer design and PCR

Four primers (PAR2 Rev, PAR2 Fwd, PK Rev and PK Fwd) were designed with overlap to the other plasmid according to ***Figures 9A-B*** based on a GC content of 40-60%, GC nucleotides present at the 3'-end to promote binding, mispriming to assure primers don't bind to multiple regions, self ΔG values to ensure no primer secondary structure and correct design of PAR2-PK plasmids using Benchling. Annealing temperatures were evaluated using NEB T_m calculator. A point mutation was induced by PAR2 rev on the PAR2 (V5)-PK assemblies for the last nucleotide of PAR2, from a T to a C, still resulting in the same amino acid (tyrosine) after translation. This was done to be able to use the PAR2 primers for all V5 and His PAR2 plasmids. Primer sequences can be found in ***Appendix F1***.

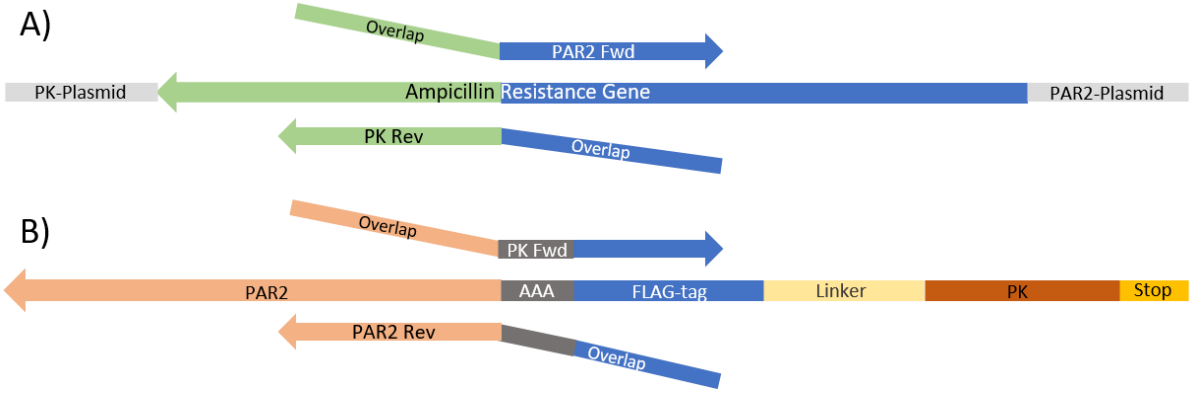

Figures 9A-B. A) The design of primers PAR2 Fwd and PK Rev over the ampicillin resistance gene. B) The design of primers PAR2 Rev and PK Fwd over the fusion between PAR2, AAA-linker, FLAG-tag, GGSGGGSGG-linker and PK followed by stop codon.

An annealing temperature optimization was done for these four primers for a gradient of 55-65°C and a 2-step PCR with annealing temperature at 72°C using PK primers and PAR2 primers respectively to obtain PK fragments and PAR2 fragments. This was done according to 50µL NEB PCR Protocol for Phusion® High-Fidelity DNA Polymerase, see ***Appendix G*** for thermocycling conditions. 20µL of each PCR reaction and 15µL E-gel 1 Kb Plus DNA ladder were loaded into a precast 1.2% E-gel with SYBR Safe and run for 26 minutes using E-Gel® iBase™ to separate products. Desired fragments from gel were 2972 bp, 2938 bp and 3721 bp from PAR2 V5 plasmids, PAR2 His plasmids and PK-plasmid respectively.

The optimal 2-step PCR 50µL reaction was then used to create necessary PK- and PAR2 fragments from PAR2 plasmid and PK-plasmid with overlapping regions. The fragments were purified with NEB Monarch® gel extraction kit according to protocol except 11000 rpm was used to elute DNA. The DNA content of fragments were then measured using NanoDrop.

3.7 Plasmid construction

3.7.1 Gibson Assembly

Nine different Gibson assembly reactions (WT (V5)-PK, E232A-PK, Y323F-PK, Y326A-PK, Y323A-PK, WT (His)-PK, Y82F-PK, D228A-PK and E232R-PK) between PK fragments and PAR2 fragments were carried out according to NEB Gibson Assembly Protocol® except a total volume of 10µL was used, see ***Appendix D3*** for WT (V5)-PK plasmid assembly example.

3.7.2 Transformation to One Shot® TOP10 competent cells

The Gibson reactions were then diluted 1:4 with water and transformed into One Shot® TOP10 competent cells where 25µL cells were used for each transformation. 2µL of diluted ligation reaction was added to the vial of competent cells prior incubation on ice for 30 minutes. The vials were then heat shocked for exactly 30 seconds in 42°C water bath allowing plasmids to enter the cells and placed on ice. 250µL SOC media was then added to each vial and the vials were shaken at 37°C for 1 hour at 300 rpm in a shaking incubator. 150µL of transformation mixture was spread on a corresponding carbenicillin plate (selection for ampicillin resistance gene) and put in an incubator at 37°C overnight. Two or three colonies were selected from each plate and each colony was inoculated in a 14mL Falcon tube with 5mL LB-media containing 100µg/mL carbenicillin overnight at 37°C and 150 rpm to obtain more plasmid DNA. The plates were left to regrow overnight at room temperature.

3.7.3 Plasmid Extraction

The plasmid DNA was extracted using NEB Monarch® Plasmid Miniprep kit following manufacturer's instructions except that the 14mL Falcon tubes were centrifuged for 2 minutes at 3700rpm as first step and DNA was eluted with 50µL nuclease-free water. The plasmid concentrations and purity were measured by NanoDrop. More plasmid DNA were obtained using PureLink HiPure Plasmid Midiprep Kits (Thermo fisher Scientific) after plasmid verification (***Section 3.7.4***). The midipreps were done following manufacturer's instructions except: 40mL of an 100mL overnight culture (LB and 100µg/mL carbenicillin) was used; after adding precipitation buffer centrifugation was at 4000g at 30 minutes; isopropanol precipitation and ethanol washing were done in 2mL Eppendorf tubes at 16000g and the DNA pellet was resuspended on 100µL nuclease-free water. The plasmid DNAs were then measured with NanoDrop and heat inactivated at 65°C for 20 minutes prior transfection.

3.7.4 Plasmid Verification

After plasmid miniprep extractions, enzyme digestion reactions of 1µL of FastDigest ScaI, 2µL FastDigest buffer (10X), 100-900 ng plasmids (including controls WT (V5), WT (His) and PK-plasmid) and water were prepared to a volume of 20µL. The digestion reactions were then incubated for 30 minutes at 37°C allowing ScaI to cut DNA. The reaction mixtures and 15µL E-gel 1 Kb Plus DNA ladder were loaded to a precast 1.2% E-gel and run for 26 minutes using E-Gel® iBase™.

PAR2 plasmids with the expected bands were then selected for sequencing for the overlapping region between PAR2 and PK fragment according to ***Figure 10***. 5µL of plasmid DNA at 80-100 ng/µL and 5µL of primer at 5µM prepared and sent to GATC Biotech for Sanger sequencing, see ***Appendix F2*** for sequencing primers.

Figure 10. Sequencing primer complements at the end of PAR2 used for sequencing over the PAR2-PK fusion region.

3.7.5 Glycerol stock formation

Colonies containing correct plasmids after plasmid verification were picked and inoculated in 5mL of LB-media containing 100µg/mL carbenicillin overnight at 37°C and 150 rpm in 14mL Falcon tubes. Glycerol stocks, stored at -80°C, were then made using 500µL overnight inoculation culture together with 500µL of 40% sterilized glycerol for future plasmid extractions. The glycerol stocks were used to scrape frozen bacteria with a sterile inoculation

loop before spreading onto carbenicillin plates. From these plates colonies were picked, inoculated and plasmids extracted (see ***Section 3.7.3***) to obtain more plasmid DNA.

3.8 Transient Transfections

50 million 1321N1 β-arrestin-EA cells were seeded in a 2 layer stack one day prior to transfection to ensure cells in growth phase. On the transfection day the media was removed and cells were washed with PBS before detachment with Accutase® and addition of media according to ***Table 3***. The cells were then transferred to a 50mL Falcon tube and counted using a Cedex HiRes analyzer prior centrifugation at 250g for 5 minutes. The supernatant was discarded and the cells were resuspended in MaxCyte electroporation buffer at 3X of the final volume (see ***Equation 4)*** and centrifuged again at 250g for 5 minutes.

$$Final\ volume = \frac{Total\ volume\ of\ cells}{Desired\ cell\ density\ (\frac{cells}{mL})} \qquad \textbf{Equation 4}$$

The cells were then resuspended with MaxCyte electroporation buffer to give a final volume such that the desired cell density of 1×10^8 cells/mL was achieved. A 50X dilution was made and counted in Cedex HiRes analyzer to ensure correct cell density. 5µg of heat inactivated plasmid DNA was then mixed with 100µL cells and added to their corresponding OC-100 cuvettes prior electroporation in MaxCyte STX with an optimized transfection protocol for 1321N1 cells. After electroporation cells were transferred to a corresponding well of a 12-well plate and incubated at 37°C for 15 minutes allowing cells to recover. 200µL of preheated DMEM GlutaMAX^{TM} media with 10% FBS was added to resuspend the cells and the cells were transferred to a corresponding 50mL Falcon tube to a total volume of 10mL media. The cells were then counted in a Cedex HiRes analyzer and centrifugated at 250g for 5 minutes. The cell pellets were resuspended in cryomedia (DMEM GlutaMAX^{TM} media with 20% FBS and 5% DMSO) for each 1321N1 β-arrestin-EA cells transfected with PAR2-PK plasmids. The resuspension was done to be able to seed 4000 cells/well in a 384 well format (i.e. ≥ 2.5M cells/cryovial). The cryovials were then placed in a Stratagene freezing box and -80°C freezer allowing gradient temperature cooling prior placement in -120°C freezer.

4 Results

4.1 β-arrestin recruitment assay on U2OS PAR2-PK/β-arrestin-EA

4.1.1 Optimization of assay window (E_{max}-E_{min})

Before beginning a study using the β-arrestin recruitment assay, parameters were optimized to maximize the assay window. The first parameter to be considered was cell number testing 2000, 3000, 4000 and 5000 cells/well. Simultaneously as cell number optimization, 0.1, 0.5, 1, 2, 3, 4, 5, and 21 hours were evaluated for the time cells were incubated with detection reagent before reading the plate. As seen in ***Figure 11***, 1 hour detection time gave the largest window for each cell number using SLIGKV as agonist.

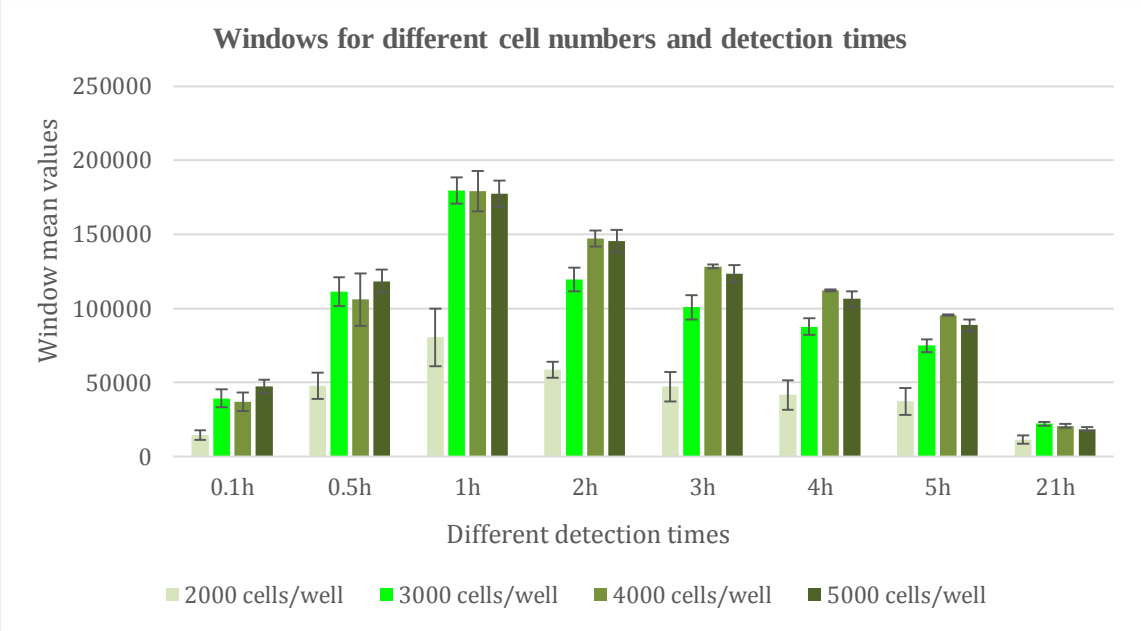

Figure 11. Windows (E_{max}-E_{min}) represented by mean±SEM based on biological triplicate measurements for cell numbers 2000, 3000, 4000 and 5000 cells/well at detection times 0.1, 0.5, 1, 2, 3, 4, 5, and 21 hours for β-arrestin recruitment using SLIGKV as agonist. SEM for each window mean is presented with an error bar.

Figure 12 shows the concentration-response curves of SLIGKV measured at 1 hour detection time with the corresponding potency data visualized in ***Table 5***.

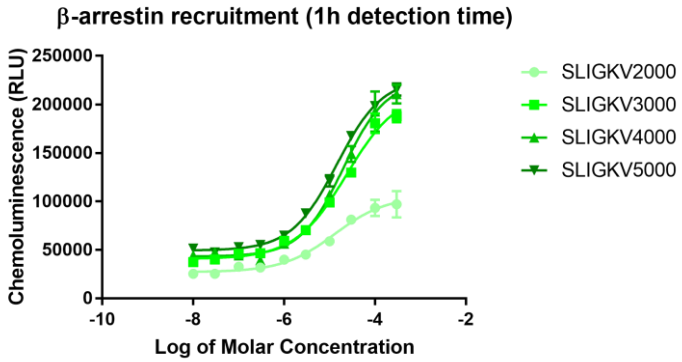

Figure 12. Concentration-response curves for 2000, 3000, 4000, and 5000 cells/well at 1 hour detection time for agonist SLIGKV in β-arrestin recruitment. SEM values are indicated with error bar for each efficacy mean value based on biological triplicate measurements.

Similar responses were seen for 4000 and 5000 cells/well and so 4000 cells/well was chosen to carry forward to optimize agonist incubation time.

Table 5. EC_{50}, E_{max}±SEM and pEC_{50}±SEM based on mean values of SLIGKV biological triplicate measurements for different cell numbers (2000, 3000, 4000 and 5000 cells/well) at 1 hour detection time for β-arrestin recruitment.

Agonist	EC_{50}	pEC_{50} ± SEM	E_{max} ± SEM
SLIGKV 2000 cells	1.81E-5	4.842 ± 0.210	109130 ± 19392
SLIGKV 3000 cells	2.70E-5	4.591 ± 0.100	219486 ± 8935
SLIGKV 4000 cells	2.04E-5	4.691 ± 0.018	223739 ± 13720
SLIGKV 5000 cells	1.56E-5	4.821 ± 0.080	228022 ± 8831

4.1.2 Optimization of agonist incubation time

Agonist incubation times 30, 60, 90 and 120 minutes were evaluated in β-arrestin recruitment for SLIGKV using optimized parameters of cell number (4000 cells/well) and detection time (1 hour). Windows (E_{max}-E_{min}) for each incubation time are visualized in ***Figure 13*** where 30 and 120 minutes has the highest and lowest window respectively. 60 and 90 minutes agonist incubation time have approximately the same window.

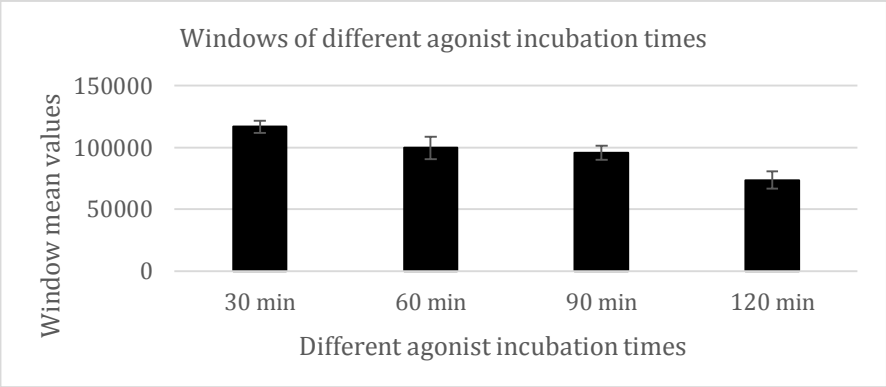

Figure 13. Windows (E_{max}-E_{min}) represented by mean±SEM based on biological triplicate measurements for SLIGKV at agonist incubation times 30, 60, 90 and 120 minutes in β-arrestin recruitment.

The potencies of SLIGKV for each agonist incubation time are visualized in ***Table 6*** where the corresponding concentration-response curves are visualized in **Figure *14***.

Table 6. EC_{50}, E_{max}±SEM and pEC_{50}±SEM based on mean values of SLIGKV biological triplicate measurements for β-arrestin recruitment at agonist incubation times 30, 60, 90 and 120 minutes.

Agonist	EC_{50}	pEC_{50} ± SEM	E_{max} ± SEM
SLIGKV 30min	2.67E-5	4.574 ± 0.019	166010 ± 4881
SLIGKV 60min	1.49E-5	4.830 ± 0.041	139210 ± 8950
SLIGKV 90min	1.13E-5	4.948 ± 0.030	132908 ± 5800
SLIGKV120min	1.08E-5	4.978 ± 0.074	101915 ± 6895

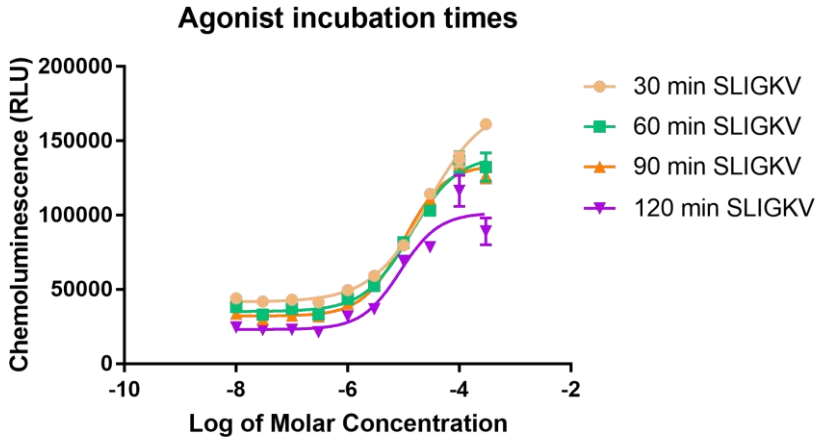

Figure 14. Concentration-response curves with efficacies and SEM values based on biological triplicate measurements for SLIGKV at different agonist incubation times (30, 60, 90 and 120 minutes) with 4000 cells/well and 1 hour detection time. SEM values are visualized with error bars.

The potency increased with longer incubation time. This is also visualized in ***Figure 15*** where the pEC_{50} reaches a plateau when increasing agonist incubation time with similar

pEC_{50} values for 90 and 120 minutes. Therefore, 90 minutes of agonist incubation time was chosen as optimized for further β-arrestin recruitment assays.

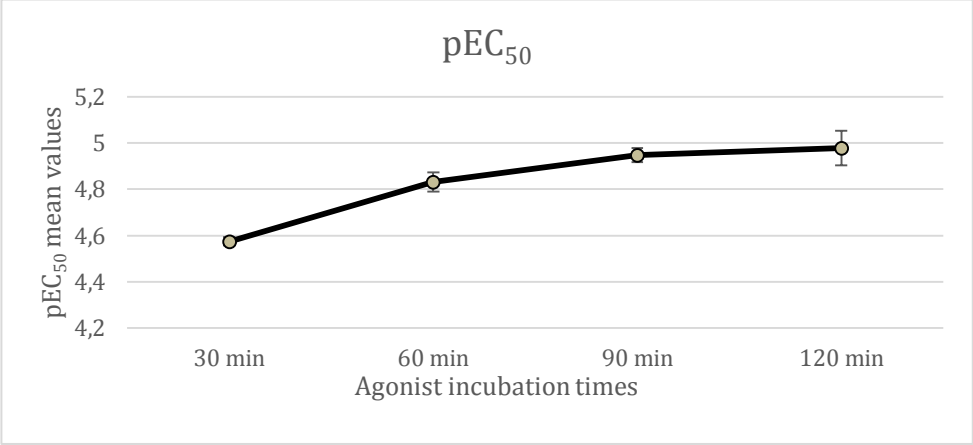

Figure 15.pEC_{50} represented by mean±SEM based on SLIGKV biological triplicate measurements for β-arrestin recruitment at agonist incubation times 30, 60, 90 and 120 minutes. SEM values are indicated by error bars for each pEC_{50} mean.

4.2 Recloning of PAR2-PK plasmids

4.2.1 Annealing temperature optimization

To be able to get higher concentrations of PAR2 and PK fragments a primer annealing temperature optimization was carried out. Firstly, a 55-65°C gradient PCR was performed for WT (V5) plasmid, WT (His) plasmid and PK-plasmid visualized in ***Figure 16***. Expected fragments from WT (V5) plasmid, WT(His) plasmid and PK-plasmid were 2972 bp, 2938 bp and 3721 bp respectively.

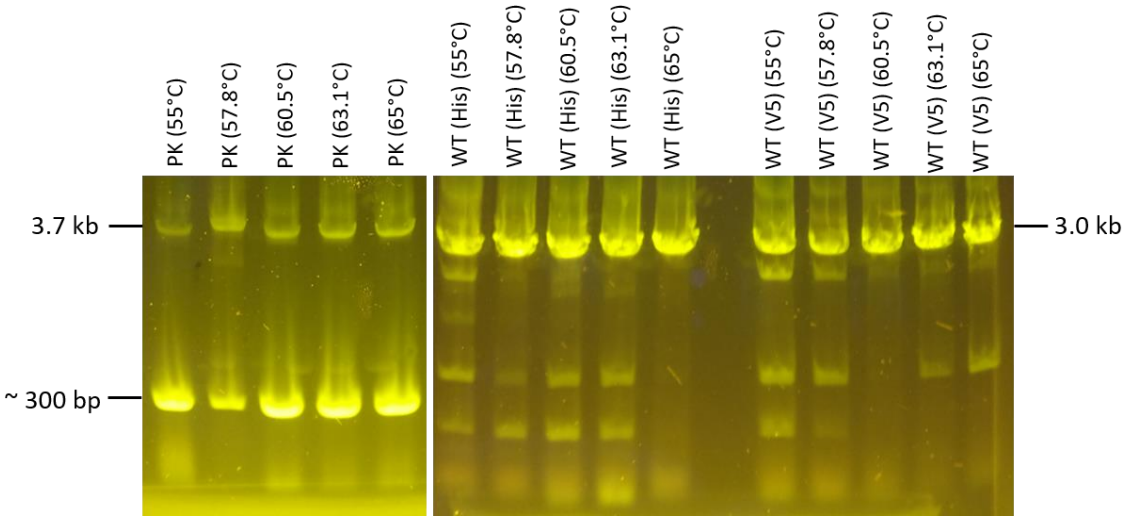

Figure 16. 55-65°C gradient PCR gel for left) PK-plasmid and right) WT (V5) plasmid and WT (His) plasmid to obtain expected fragments of approximately 3700 bp, 3000 bp and 3000 bp from PK-plasmid, WT (V5) plasmids and WT (His) plasmids respectively.

Since there were non-desired fragments from PAR2- and PK-plasmids a 2-step PCR was evaluated. The gel of the 2-step PCR is visualized in ***Figure 17***. Fewer non-specific bands for PAR2 plasmids were seen and a higher intensity of PK-fragment was obtained. Therefore, the 2-step PCR was chosen for future PCRs.

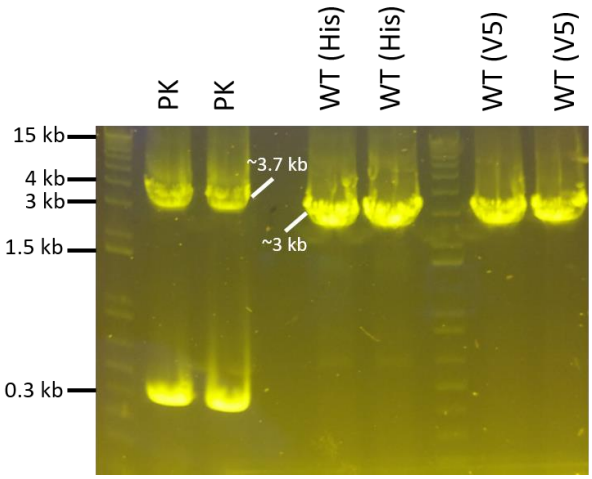

Figure 17. 2-step PCR for PK-plasmid, WT (V5) plasmid and WT (His) plasmid. Expected bands of approximately 3.7 kb and 3 kb were seen for PK-plasmid and WT (His) and (V5) plasmids respectively. E-Gel 1 Kb Plus DNA ladder was used as DNA ladder.

4.2.2 Evaluation of plasmids

The number of colonies for WT (V5)-PK, E232A-PK, Y323F-PK, Y326A-PK, Y323A-PK, WT (His)-PK, Y82F-PK, D228A-PK and E232R-PK on carbenicillin plates after Gibson assembly and transformation to One Shot® TOP10 competent cells were estimated to 58, 64, 81, 31, 53, 85, 104, 27 and 26 respectively. Two colonies from each of these plates were selected for ScaI restriction enzyme digestion to evaluate the plasmids, where expected base pairs of products are found in ***Table 7***. ***Figure 18*** visualizes a representative example, showing ScaI digestion of E232A-PK, Y323F-PK and Y323A-PK. For WT (V5)-PK, Y326A-PK, WT (His)-PK, Y82F-PK, D228A-PK and E232R-PK digestions, see ***Appendix H***.

Table 7. Expected bands of PAR2 (V5)-PK, PAR2 (His)-PK, WT (V5) control, WT (His) control and PK-plasmid control after ScaI enzyme digestion.

Plasmids	Number of fragments	Fragment lengths (bp)
PAR2 (V5)-PK Mut + WT	2	3761+2852
PAR2 (His)-PK Mut + WT	2	3761+2818
PAR2 (V5) WT Control	1	6639
PAR2 (His) WT Control	1	6596
PK-plasmid Control	3	1564+3761+2351

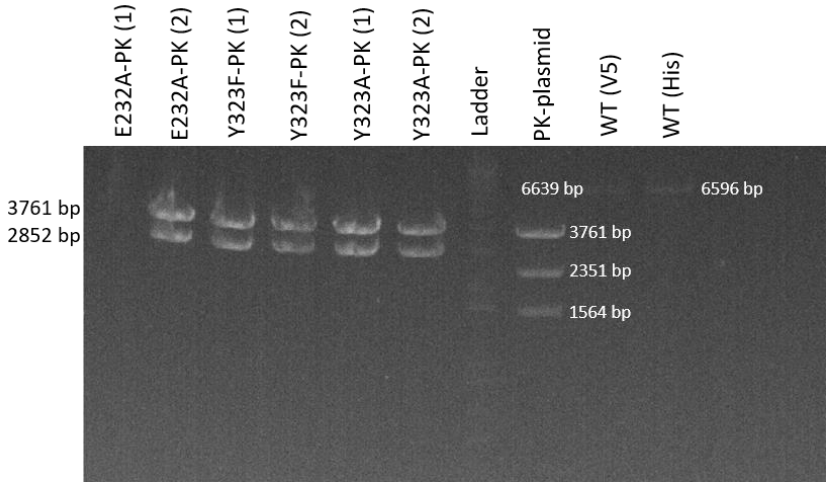

Figure 18. Gel of ScaI digestions for E232A-PK (1,2), Y323F-PK (1,2), Y323A-PK (1,2), WT (His) control, WT (V5) control and PK-plasmid with E-Gel 1 Kb Plus DNA ladder visualized. Expected bands of PAR2-PK V5 plasmids (3761 and 2852 bp), PK-plasmid control (3761, 2351 and 1564 bp), PAR2 V5 WT (6639 bp) and PAR2 His WT (6596 bp).

One colony for each Gibson assembly showing correct ScaI digest were sent in for sequencing over the PAR2-PK fusion region using PAR2-PK WT plasmids as a template (where WT (V5)-PK template had no T to C point mutation). For visualization of sequencing results for the selected colonies, see ***Figures 19A-I***, where grey colors indicate sequence identity to while white and red regions indicate sequence non-identity. Sequence identity was observed except at the beginning and at the end of the sequencing, at the T to C point mutation for V5 assemblies and within the EMCV-IRES region. The sequence non-identity was explainable (see ***Section 5.2.2***). Therefore, these colonies were evaluated to have correctly assembled plasmids.

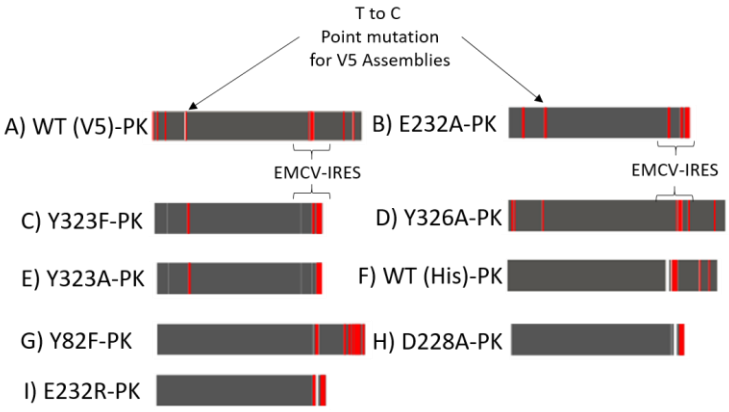

Figures 19A-I. Sequencing results of A) WT (V5)-PK, B) E232A-PK, C) Y323F-PK, D) Y326A-PK, E) Y323A-PK, F) WT (His)-PK, G) Y82F-PK, H) D228A-PK and I) E232R-PK aligned to corresponding PAR2-PK WT plasmid where the WT (V5)-PK template did not have the T to C point mutation. Sequence identity between the sequencing results and template DNA sequence is indicated by grey colors while sequence non-identity is indicated by red and white colors. T to C point mutation is shown for WT (V5)-PK, E232A-PK, Y323F-PK, Y326A-PK and Y323A-PK and the EMCV-IRES region uncertainties are seen for all PAR2-PK plasmids.

Glycerol stocks containing colonies with correct plasmids after plasmid verifications were used to obtain more plasmid DNA utilizing the PureLink HiPure Plasmid Midiprep Kit. For plasmid DNA concentrations, purities and volume after plasmid midipreps, see ***Table 8***.

Table 8. 260/280, 260/230, ng/µl and volume of plasmid DNAs for WT (V5)-PK, E232A-PK, Y323F-PK, Y326A-PK, Y323A-PK, WT (His)-PK, Y82F-PK, D228A-PK and E232R-PK after plasmid midipreps.

Plasmid	ng/µl	260/280	260/230	Volume (µl)
WT (V5)-PK	1846.6	1.88	2.27	200
E232A-PK	1556.2	1.89	2.27	100
Y323F-PK	1739.4	1.88	2.25	100
Y326A-PK	2259.2	1.88	2.28	200
Y323A-PK	1119.8	1.91	2.29	100
WT (His)-PK	940	1.89	2.30	200
Y82F-PK	1070.4	1.90	2.27	100
D228A-PK	1300.4	1.89	2.28	100
E232R-PK	1490.0	1.89	2.27	100

4.3 Evaluation of membrane expression (FLIPR)

1321N1 β-arrestin-EA cells transiently transfected with WT (V5)-PK, E232A-PK, Y323F-PK, Y326A-PK, Y323A-PK, WT (His)-PK, Y82F-PK, D228A-PK and E232R-PK were evaluated in FLIPR for agonists SLIGKV, SLIGRL, GB110 and 2f-LIGRLO to confirm membrane expression of PAR2. Commercial U2OS PAR2-PK/β-arrestin-EA and parental 1321N1 β-arrestin-EA cells were used as a positive and negative controls respectively. For concentration-response curves and potency data for FLIPR, see ***Figures 20A-L*** and ***Appendix I*** respectively.

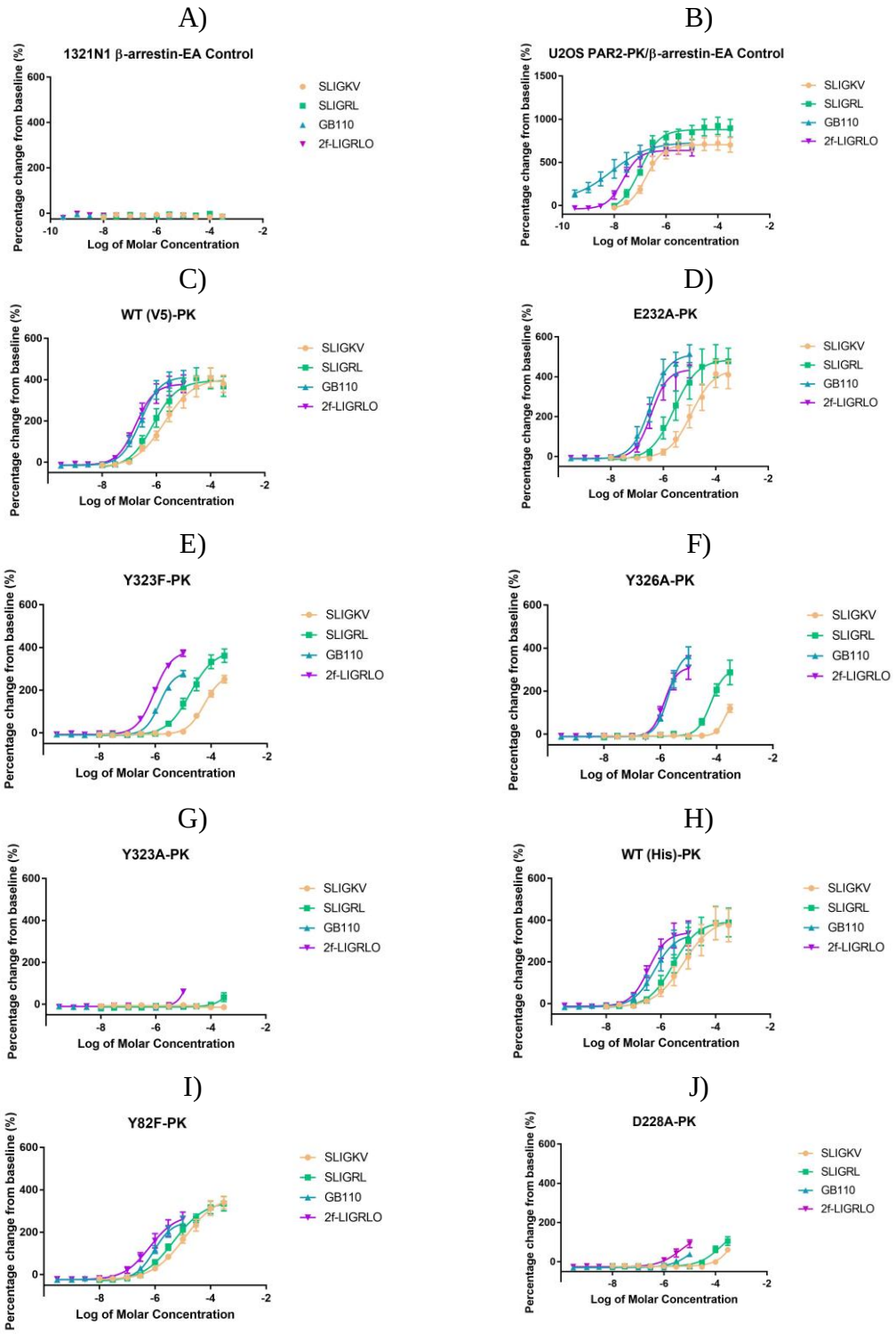

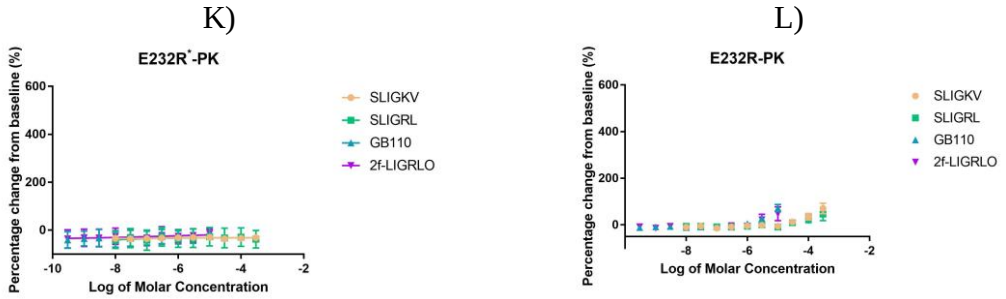

Figures 20A-L. FLIPR concentration-response curves for A) 1321N1 β-arrestin-EA cells control, B) U2OS PAR2-PK/β-arrestin-EA cells control, 1321N1 β-arrestin-EA cells with C) WT (V5)-PK, D) E232A-PK, E) Y323F-PK, F) Y326A-PK, G) Y323A-PK, H) WT (His)-PK, I) Y82F-PK, J) D228A-PK, K) E232R*-PK and L) E232-PK using agonists SLIGKV (yellow), SLIGRL (green), GB110 (blue) and 2f-LIGRLO (magenta). All curves are based on two experimental replicates each consisting of biological triplicate measurements except for E232R-PK and E232R-PK* where one experimental replicate was done each. Data presented as mean±SEM.

As seen in ***Figures 20A-L*** all (except E232*-PK) 1321N1 β-arrestin-EA cells transfected with PAR2-PK plasmids showed responses in FLIPR indicating that PAR2 was expressed at the membrane.

4.4 Western blot evaluation

To compare differences in expression levels between different 1321N1 β-arrestin-EA cells transiently transfected with WT (V5)-PK, E232A-PK, Y323F-PK, Y326A-PK, Y323A-PK, WT (His)-PK, Y82F-PK, D228A-PK and E232R*-PK, western blot was evaluated. Expression was evaluated for PAR2 but also β-actin as a loading control where 1321N1 β-arrestin-EA and a 1321N1 PAR2 control were negative and positive controls respectively, see ***Figure 21A-B***.

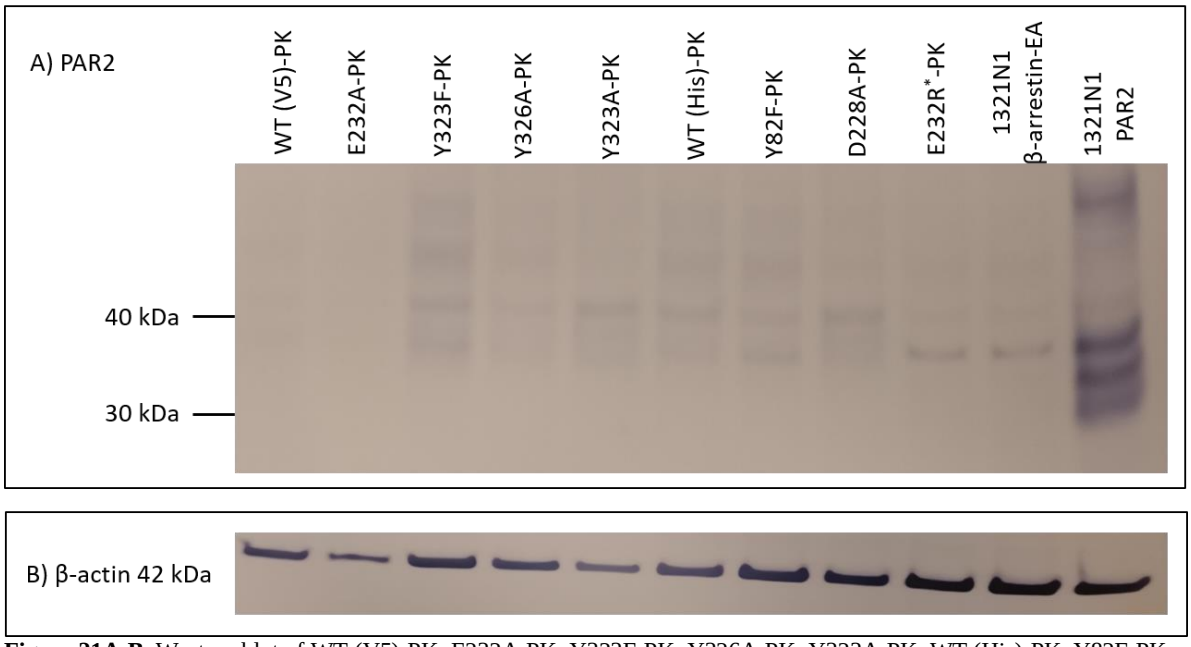

Figure 21A-B. Western blot of WT (V5)-PK, E232A-PK, Y323F-PK, Y326A-PK, Y323A-PK, WT (His)-PK, Y82F-PK, D228A-PK, E232R*-PK, 1321N1 β-arrestin-EA and 1321N1 PAR2 control for A) PAR2 and B) β-actin.

Similar amounts of total proteins were loaded into each well indicated by the β-actin loading control except for WT (V5)-PK, E232A-PK, Y326A-PK and Y323A-PK where lower intensity of bands were seen (***Figure 21B)***. For PAR2 (***Figure 21A***) similar expressions were seen for Y323F-PK, Y326A-PK, Y323A-PK, WT (His)-PK, Y82F-PK and D228A-PK with

bands larger compared to the the PAR2 control due to the addition of the PK-tag. However, no bands were seen for WT (V5)-PK and E232A-PK which could be due to less protein added to these wells indicated by the β-actin control. E232R*-PK and 1321N1 β-arrestin-EA negative control showed similar responses and thus that PAR2 is not expressed in E232R*-PK.

Because the first western blot did not show any bands for WT (V5)-PK and E232A-PK but also to see possible expression of E232R, a second western blot was made loading more cell lysate to each well, see ***Figure 22A-B***.

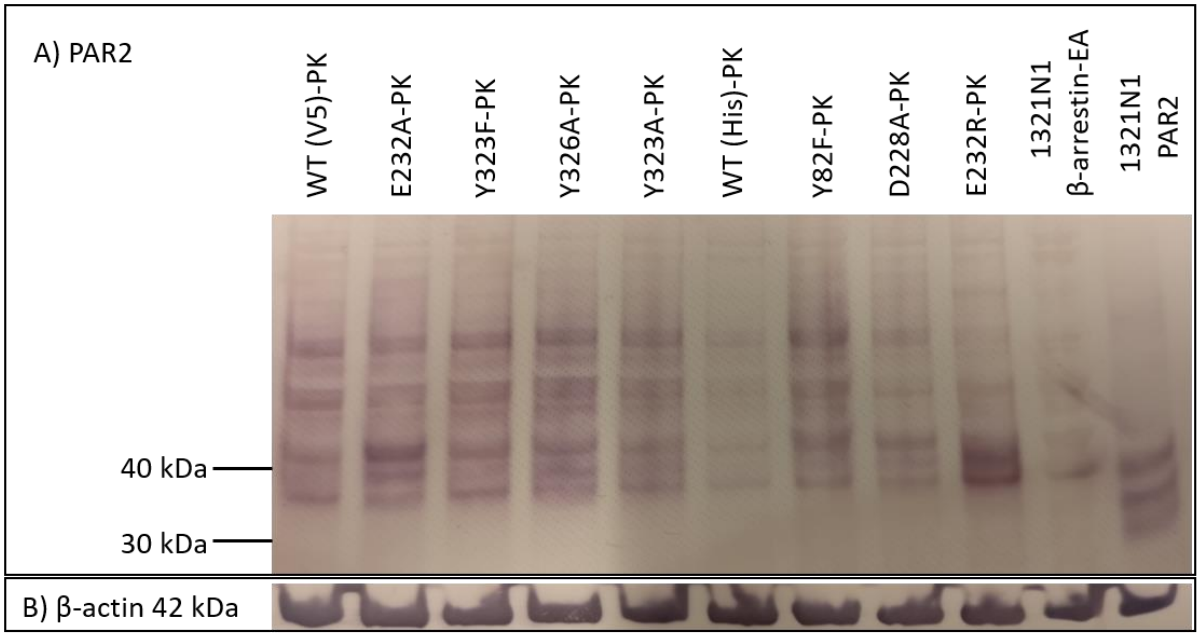

Figure 22A-B. Western blot of WT (V5)-PK, E232A-PK, Y323F-PK, Y326A-PK, Y323A-PK, WT (His)-PK, Y82F-PK, D228A-PK, E232R-PK, 1321N1 β-arrestin-EA and 1321N1 PAR2 control for A) PAR2 and B) β-actin.

As seen in **Figure *22A*** similar amount of proteins were loaded of all samples. Similar PAR2 expression (**Figure *22B***) were seen for all samples except for WT (His)-PK and D228A-PK which had lower expression. E232R-PK showed expression of PAR2 which E232R*-PK did not in the previous western blot. 1321N1 β-arrestin-EA did not show any expression of PAR2, similar to the other western blot.

4.5 Evaluation of β-arrestin recruitment

1321N1 β-arrestin-EA cells transiently transfected with WT (V5)-PK, E232A-PK, Y323F-PK, Y326A-PK, Y323A-PK, WT (His)-PK, Y82F-PK, D228A-PK and E232R-PK were evaluated in β-arrestin recruitment for agonists SLIGKV, SLIGRL, GB110 and 2f-LIGRLO to evaluate important amino acid residues of PAR2 for β-arrestin-mediated signalling. Commercial U2OS PAR2-PK/β-arrestin-EA and parental 1321N1 β-arrestin-EA cells were used as positive and negative controls respectively. For concentration-response curves and potency data for β-arrestin recruitment, see ***Figures 23A-L*** and ***Tables 9A-L*** respectively.

A) B)

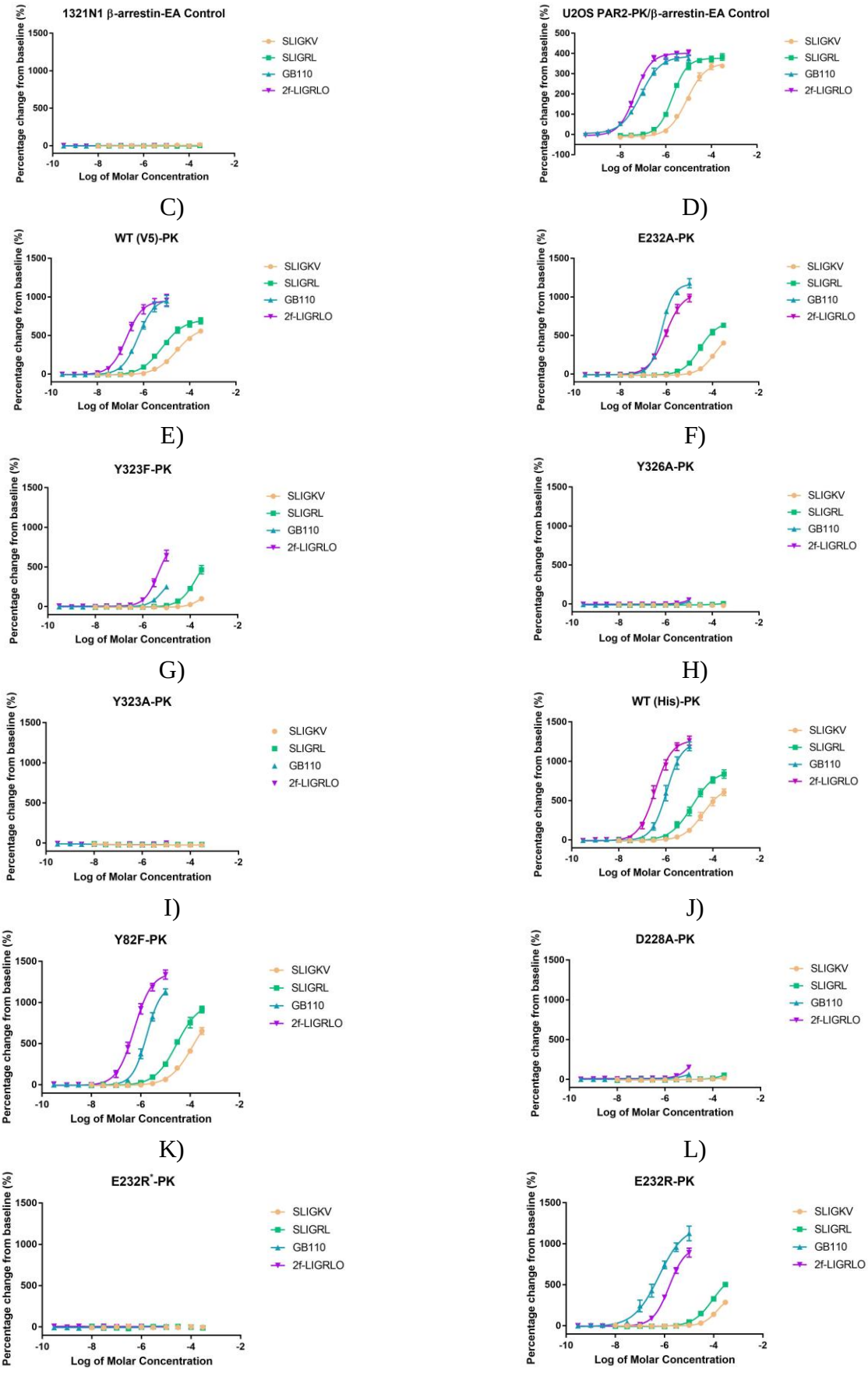

Figures 23A-L. β-arrestin recruitment concentration-response curves for A) 1321N1 β-arrestin-EA control cells, B) U2OS PAR2-PK/ β-arrestin-EA control, 1321N1 β-arrestin-EA cells with C) WT (V5)-PK, D) E232A-PK, E) Y323F-PK, F) Y326A-PK, G) Y323A-PK, H) WT (His)-PK, I) Y82F-PK, J) D228A-PK, K) E232R*-PK and L) E232R-PK using agonists

SLIGKV (yellow), SLIGRL (green), GB110 (blue) and 2f-LIGRLO (magenta). All curves are based on ≥ 3 experimental replicates each consisting of biological triplicate measurements except for E232R-PK and E232R*-PK where two experimental replicate were done each. Data presented as mean±SEM.

As seen in ***Figures 23A-L*** and ***Tables 9A-L*** different responses were seen for some mutants compared to WT PAR2-PK 1321N1 β-arrestin-EA cells. No response was seen for E232R*-PK similarly to the corresponding western blot and FLIPR results.

Tables 9A-L. EC_{50}, pEC_{50}±SEM and E_{max}±SEM for agonists SLIGKV, SLIGRL, GB110 and 2f-LIGRLO in β-arrestin recruitment based on mean values of three experimental replicates each consisting of biological triplicate measurements except for E232R*-PK and E232R-PK where two experimental replicates were carried out each. Potency tables are visualized for: A) 1321N1 β-arrestin-EA control cells, B) U2OS PAR2-PK/ β-arrestin-EA control cells, transiently transfected 1321N1 β-arrestin-EA cells with C) WT (V5)-PK, D) E232A-PK, E) Y323F-PK, F) Y326A-PK, G)Y323A-PK, H) WT (His)-PK, I) Y82F-PK, J) D228A-PK, K) E232R*-PK and L) E232R-PK. N.R indicates no response.

A) 1321N1 β-arrestin-EA Control

Agonist	EC_{50}	pEC_{50} ± SEM	E_{max} ± SEM
SLIGKV	N. R	N. R	N. R
SLIGRL	N. R	N. R	N. R
GB110	N. R	N. R	N. R
2f-LIGRLO	N. R	N. R	N. R

B) U2OS PAR2-PK/β-arrestin-EA Control

Agonist	EC_{50}	pEC_{50} ± SEM	E_{max} ± SEM
SLIGKV	9.89E-6	5.03 ± 0.046	338.30 ± 11.05
SLIGRL	2.08E-6	5.69 ± 0.028	382.67 ± 16.66
GB110	8.41E-8	7.10 ± 0.053	374.21 ± 19.25
2f-LIGRLO	4.93E-8	7.33 ± 0.045	403.54 ± 13.96

C) 1321N1 WT (V5)-PK/β-arrestin-EA

Agonist	EC_{50}	pEC_{50} ± SEM	E_{max} ± SEM
SLIGKV	3.03E-5	4.56 ± 0.050	557.95 ± 31.15
SLIGRL	7.23E-6	5.17 ± 0.041	690.03 ± 40.03
GB110	6.05E-7	6.23± 0.028	946.83 ± 72.30
2f-LIGRLO	1.94E-7	6.73 ± 0.036	959.36 ± 74.36

D) 1321N1 E232A-PK/β-arrestin-EA

Agonist	EC_{50}	pEC_{50} ± SEM	E_{max} ± SEM
SLIGKV	1.25E-4	3.94 ± 0.064	403.15 ± 22.27
SLIGRL	3.46E-5	4.51 ± 0.070	633.06 ± 31.55
GB110	6.66E-7	6.19 ± 0.031	1178.24 ± 59.79
2f-LIGRLO	1.07E-6	6.01 ± 0.064	985.94 ± 49.72

E) 1321N1 Y323F-PK/β-arrestin-EA

Agonist	EC_{50}	pEC_{50} ± SEM	E_{max} ± SEM
SLIGKV	N. R	N. R	N. R
SLIGRL	2.05E-5	3.72 ± 0.065	465.96 ± 52.72
GB110	N. R	N. R	N. R
2f-LIGRLO	5.26E-6	5.30 ± 0.055	643.46 ± 67.96

F) 1321N1 Y326-PK/β-arrestin-EA

Agonist	EC_{50}	pEC_{50} ± SEM	E_{max} ± SEM
SLIGKV	N. R	N. R	N. R
SLIGRL	N. R	N. R	N. R
GB110	N. R	N. R	N. R
2f-LIGRLO	N. R	N. R	N. R

G) 1321N1 Y323A-PK/β-arrestin-EA

Agonist	EC_{50}	pEC_{50} ± SEM	E_{max} ± SEM
SLIGKV	N. R	N. R	N. R
SLIGRL	N. R	N. R	N. R
GB110	N. R	N. R	N. R
2f-LIGRLO	N. R	N. R	N. R

H) 1321N1 WT (His)-PK/β-arrestin-EA

Agonist	EC_{50}	pEC_{50} ± SEM	E_{max} ± SEM
SLIGKV	4.85E-5	4.40 ± 0.098	605.40 ± 42.06
SLIGRL	2.02E-5	4.82 ± 0.114	837.91 ± 53.11
GB110	1.28E-6	5.96 ± 0.086	1189.38 ± 56.46
2f-LIGRLO	3.83E-7	6.45 ± 0.058	1261.74 ± 57.89

I) 1321N1 Y82F-PK/β-arrestin-EA

Agonist	EC_{50}	pEC_{50} ± SEM	E_{max} ± SEM
SLIGKV	1.07E-4	4.00 ± 0.058	654.43 ± 41.62
SLIGRL	3.27E-5	4.51 ± 0.046	914.89 ± 39.90
GB110	1.85E-6	5.76 ± 0.057	1130.15 ± 36.36
2f-LIGRLO	6.25E-7	6.26 ± 0.080	1338.76 ± 56.13

J) 1321N1 D228A-PK/β-arrestin-EA

Agonist	EC_{50}	pEC_{50} ± SEM	E_{max} ± SEM
SLIGKV	N. R	N. R	N. R
SLIGRL	N. R	N. R	N. R
GB110	N. R	N. R	N. R
2f-LIGRLO	N. R	N. R	N. R

K) 1321N1 E232R*-PK/β-arrestin-EA

Agonist	EC_{50}	pEC_{50} ± SEM	E_{max} ± SEM
SLIGKV	N. R	N. R	N. R
SLIGRL	N. R	N. R	N. R
GB110	N. R	N. R	N. R
2f-LIGRLO	N. R	N. R	N. R

L) 1321N1 E232R-PK/β-arrestin-EA

Agonist	EC_{50}	pEC_{50} ± SEM	E_{max} ± SEM
SLIGKV	N. R	N. R	N. R
SLIGRL	1.05E-4	4.02 ± 0.079	503.92 ± 30.74
GB110	6.06E-7	6.27 ± 0.101	1126.07 ± 89.80
2f-LIGRLO	1.76E-7	5.78 ± 0.064	892.67 ± 54.20

Since differences in responses were seen between mutant and wild type receptors, fold change was evaluated. It was calculated by dividing the geometric EC_{50} mean value of the mutant receptor with the geometric EC_{50} mean value of the corresponding wild type receptor, see **Table *10***, where a larger fold change indicates a reduction in potency.

Table 10. Fold change between wild type 1321N1 β-arrestin-EA/PAR2-PK (WT (V5)-PK and WT (His)-PK) and mutants E232A-PK, Y323F-PK, Y326A-PK, Y323A-PK, Y82F-PK, D228A-PK and E232R-PK calculated by divding geometric EC_{50} mean values of mutant receptor by the corresponding geometric EC_{50} mean value of wild type receptor.

Fold Change	WT (V5) PK	E232A PK	Y323F PK	Y326A PK	Y323A PK	WT (His) PK	Y82F PK	D228A PK	E232R PK
SLIGKV	1	4.16	>10.92	>10.92	>10.92	1	2.55	>7.61	>7.61
SLIGRL	1	4.55	27.78	>44.15	>44.15	1	2.08	>19.99	6.40
GB110	1	1.11	>17.01	>17.01	>17.01	1	1.58	>9.16	0.49
2f-LIGRLO	1	5.34	27.10	>54.16	>54.16	1	1.55	>28.07	4.68

5 Discussion and Conclusions

5.1 Optimization of β-arrestin recruitment assay

The chart in ***Figure 11*** provides a clear result of 1 hour as a preferred detection time where 3000, 4000, 5000 cells/well have similar windows. The window of 3000 cells/well is not similar to 4000 or 5000 cells/well after 1 hour detection whereas 4000 or 5000 cells have similar windows for all detection times. As seen in ***Table 5***, EC_{50} changes depending on cell number where 3000 cells/well has a higher EC_{50} value compared to other cell numbers at this detection time. 4000 cells/well was chosen as the optimized cell number as it gave a similar response to 5000 cells/well and it is a waste to use more cells than necessary. The concentration-response curves look similar for 3000, 4000 or 5000 cells/well but these differs greatly from 2000 cells/well as seen in ***Figure 12***.

For agonist incubation time (see **Figure *15***) the pEC_{50} reached a plateu at 90 minutes incubation time. This indicates equilibrium is reached, a requirement for the mathematical model obtaining concentration-response curves. Therefore, an agonist incubation time of 90 minutes was chosen as optimal.

The optimized conditions were only determined doing the experiment once with three biological replicates. With more experimental replicates it would be possible to obtain more statistically significant results. The first experiment also had a fixed value of agonist incubation time of 90 minutes which could effect the optimization results if optimized parameters are dependent on each other. Due to time constraints, the clear results from one experimental replica and the consistency of optimization results that previously were found in the lab by others; these optimized conditions were taken forward and no further optimization experiments were carried out.

Since optimization of the β-arrestin recruitment assay was done on the U2OS cell line it could be possible that the used 1321N1 β-arrestin-EA cell line transfected with PAR2-PK plasmids does not share the same optimized conditions. However, the U2OS cell line is commercial, has been quality controlled and should therefore work in the β-arrestin recruitment assay. Thus, the U2OS cell line serves as a good control for the transiently transfected 1321N1 cells with PAR-PK plasmids.

5.2 Recloning of PAR2 plasmids

5.2.1 Annealing temperature optimization

In ***Figure 16*** clear bands were seen for both plasmids WT (V5) PAR2- and WT (His) PAR2 plasmids approximately 3000 bp at all temperatures but unspecific binding of primers seems to take place at lower temperatures resulting in more bands. When increasing the temperature, primers seem to bind more specifically and thus fewer bands were seen on gel. Due to this a 2-step PCR was evaluated. For PK-plasmid the wanted fragment of 3700 bp has

a low intensity which could be due to possible hetero-primer dimerization or mispriming resulting in a smaller higher intensity fragment at approximately 300 bp. Primers were evaluated for mispriming before use indicating this shouldn't be happening. However, an evaluation of possible primer hetero-dimerization between the two PK primers was not carried out before ordering the primers but was done later indicating that primer hetero-dimerization is possible to have happened.

The 2-step PCR, visualized in ***Figure 17***, showed a higher intensity of the wanted PK-fragment and no unspecific binding of primers in the case of PAR2 plasmids. Still, there were possible primer dimerization or mispriming seen in the case of PK-plasmid similar to the gradient PCR. Correct PCR fragments with sufficient intensity for Gibson assembly were obtained; thus the 2-step PCR was used in further PCRs to obtain fragments ready for Gibson assemblies.

5.2.2 Evaluation of plasmids

Since colonies were found on the carbenicillin plates for all Gibson assemblies this suggested that the Gibson assemblies and transformations to One Shot® TOP10 competent cells were successful. This is a result of the cells expressing ampicillin resistance obtained from Gibson assembly using the overlaps from PAR2 Fwd and PK Rev, see ***Figures 9A-B***.

The results from sequencing, see ***Figures 19A-I***, showed PAR2 and the PK fragment to be in frame according to ***Figure 10*** indicating that the construction of plasmids were successful. The sequencing results also verfied that the V5/His Gibson assemblies originated from the PAR2 V5/His plasmids due to their sequence identity compared with the corresponding template sequence. For example, WT (V5)-PK, E232A-PK, Y323F-PK and Y326A-PK and Y323A-PK sequencing results showed that the desired point mutation from a T to C had taken place. This indicated that the PAR2 primers can be used for all PAR2 His- and PAR2 V5 plasmids. Some uncertainty in sequencing results were found at the beginning, at the end of the sequencing and in the EMCV-IRES region. This could be due to Sanger sequencing can result in poor quality at the beginning and the end of the sequencing results but also within the EMCV-IRES region due to repetitive cytosines making it difficult to see sequence differences (Sanger et al., 1977).

5.3 Confirmation of surface expression of PAR2 (FLIPR)

As seen in ***Figures 20A-L*** all (except E232R*-PK) 1321N1 β-arrestin-EA cells with PAR2-PK plasmids showed responses in inositol phospholipid pathway indicating PAR2 is expressed, activated and that it is located at the membrane. The responses also suggest that some of the point mutations affect the G_q-mediated signalling more than others. For example Y323A-PK, D228A-PK and E232R-PK show lower responses than other mutants. Still, more experimental replicates are needed to obtain more statistically significant results.

The FLIPR potency data for the 1321N1 β-arrestin-EA PAR2-PK wild types and U2OS control cell lines, seen in ***Appendix I,*** showed that GB110 and 2f-LIGRLO have similar potencies and higher compared to SLIGKV and SLIGRL that have similar potencies. This data for GB110, 2f-LIGRLO, SLIGKV and SLIGRL agrees with published literature (Suen et al., 2012, Kanke et al., 2009). The potency data also showed that transiently transfected 1321N1 β-arrestin-EA with wild type PAR2-PK receptors were shifted compared to the U2OS cell control. The shift between 1321N1 PAR2 WT β-arrestin-EA cell lines and the U2OS cell line is most likely due to different expression levels of PAR2.

5.4 Western blot

As seen in ***Figure 21A-B*** less intense bands of β-actin were seen for WT (V5)-PK and E232A-PK and no appearent bands were observed the PAR2 membrane. A reason for this could be that when resuspending these cells no cell pellets were visible indicating a loss of cells must have taken place during western blot sample preparation. Therefore, another western blot was made showing the expression of WT (V5)-PK and E232A-PK (***Figure 22B***).

Transient transfection of each PAR2-PK plasmid into 1321N1 β-arrestin-EA cells was carried out on two separate occasions. In the case of the E232R-PK plasmid after one transfection, there was no response of the cells in either FLIPR or β-arrestin recruitment (E232R*-PK) while after the second transfection there was (E232R-PK). Therefore, E232R*-PK was expected to show no PAR2 expression in the western blot similar to the 1321N1 β-arrestin negative control which was observed. Thus, only results from E232R-PK 1321N1 β-arrestin-EA cells (which showed PAR2 expression in ***Figure 22B***) were considered when looking into fold change compared to wild type WT (His)-PK 1321N1 β-arrestin-EA cells.

5.5 Evaluation of β-arrestin recruitment

As seen in ***Figures 23A-L*** the 1321N1 β-arrestin-EA control cell line showed no response for all agonists suggesting that all possible responses seen in this cell line were due to the transfections with PAR2-PK plasmids. Responses in β-arrestin recruitment were seen and different responses were seen for some of the point mutated PAR2s suggesting important residues for activation of β-arrestin-mediated signalling by agonists SLIGKV, SLIGRL, GB110 and 2f-LIGRLO. The responses indicated that the PK-tag had been succesfully placed at the C-terminus of PAR2 and that PAR2-PK was functional. For structural formulas of amino acids focused on during this project, see ***Appendix C***.

5.5.1 Wild types

U2OS PAR2-PK/β-arrestin-EA cells showed similar concentration-response curves to 1321N1 β-arrestin-EA transiently transfected with WT (V5)-PK and WT (His)-PK where 2f-LIGRLO and GB110 were equipotent but more potent than SLIGKV and SLIGRL which were also equipotent. The U2OS PAR2-PK/β-arrestin-EA had higher potencies of all agonists compared to 1321N1 β-arrestin-EA wild type receptor cell lines which is also consistent in the FLIPR potency data (***Appendix I***). This is possibly due to different expression levels of PAR2. Similar potencies for agonists were seen for 1321N1 β-arrestin-EA WT (V5)-PK and WT (His)-PK cell lines. Another difference of the U2OS control compared to the 1321N1 β-arrestin-EA PAR2 wild types cells was that SLIGKV and SLIGRL look to be partial agonists in the 1321N1 β-arrestin-EA PAR2 wild type cell lines. One suggestion to explain this is that DiscoverX might have used different linkers in the PAR2-PK fusion region. This could result in different functionalities of the PAR2-PK fusion which might result in slight differences in E_{max} of SLIGRL and SLIGKV compared to GB110 and 2f-LIGRLO.

5.5.2 E232

E232 (negatively charged glutamic acid) located on the ECL2 of PAR2 was exchanged for an uncharged alanine (E232A-PK) and a positively charged arginine (E232R-PK). As seen in ***Figures 23*** and ***Tables 9*** C,D, H and L some differences were seen depending on agonist and point mutation. The fold changes in ***Table 10*** suggest that SLIGKV, SLIGRL and 2f-LIGRLO prefer the negatively charge E232 because a positive or uncharged residue results in higher EC_{50} values compared to the wild type case. This suggests that E232 is of importance

in β-arrestin-mediated signalling for SLIGKV, SLIGRL and 2f-LIGRLO. A hypothesis to this could that SLIGKV has a positively charged K (lysine) while SLIGRL and 2f-LIGRLO have a positively charged R (arginine) which makes these prefer the negatively charged glutamic acid. Change of E232 residue to an uncharged or positively charged residue does not seem to be important for GB110. A hypothesis to this is that GB110 is not charged and thus should not depend on charge of the E232 residue.

5.5.3 Y323

Y323 (tyrosine) has a hydroxyl group which was exchanged to phenylalanine that has no hydroxyl group (Y323F-PK) and to alanine that has no hydroxyl group and is less bulky (Y323A-PK). As seen in ***Figures 23***, ***Tables 9*** C,E and G and fold change ***Table 10*** the exchange to an phenylalanine resulted in reduced potency for all agonists which suggest the importance of a hydroxyl group of Y323. A hypothesis to this could be that the hydroxyl group of Y323 forms a hydrogen bond with the agonists and is therefore preferred for PAR2 to induce β-arrestin-mediated signalling. The exchange from Y323 to an alanine results in no response of agonists in β-arrestin recrutment suggesting the importance of a bulky residue of PAR2 at amino acid 323. These results suggest the importance of Y323 in β-arrestin-mediated signalling for agonists SLIGKV, SLIGRL, GB110 and 2f-LIGRLO.

5.5.4 Y82

Y82 (tyrosine) was bound to the antagonist AZ8838 in the solved crystal structure indicating this is a possible important residue in binding of other molecules such as agonists. Y82 has a hydroxyl group and was exchanged to phenylalanine (Y82F-PK), see ***Figures 23***, ***Tables 9*** H and I and fold change **Table *10***. As seen in ***Table 10*** there were similar potencies between Y82F-PK and WT (His)-PK for all agonists where the agonists were slightly more potent in WT (His)-PK compared to Y82F-PK. It could be that the point mutation induces this shift although it is not significant according to the results. Thus, Y82 could be of importance in β-arrestin-mediated signalling but the results doesn't suggest that it significantly is. Therefore, the data suggest the hydroxyl group of Y82 is not important inducing β-arrestin-mediated signalling of agonists SLIGKV, SLIGRL, GB110 and 2f-LIGRLO.

5.5.5 D228

D228, a negatively charged aspartic acid, was like Y82 bound to the antagonist AZ8838 in the solved crystal structure. This residue was exchanged to alanine which is less bulky and uncharged (D228A-PK). As seen in ***Figures 23***, ***Tables 9*** H and J and fold change ***Table 10*** no responses and no obtainable EC_{50} values were observed for the agonists. Therefore, this suggests that D228 is of importance in β-arrestin-mediated signalling for agonists SLIGKV, SLIGRL, GB110 and 2f-LIGRLO.

5.5.6 Y326

Y326, tyrosine, was exchanged to alanine which has no hydroxyl group and is less bulky (Y326A-PK). ***Figures 23***, ***Tables 9*** C and F and fold change ***Table 10*** no responses and no obtainable EC_{50} values were observed for the agonists. This indicates that Y326 is of importance in β-arrestin-mediated signalling for agonists SLIGKV, SLIGRL, GB110 and 2f-LIGRLO.

6 Conclusions

The optimized conditions for the β-arrestin recruitment assay was found to be 4000 cell/well, 90 minutes of agonist incubation time and 60 minutes of detection time. PAR2 agonists (2f-LIGRLO, GB110, SLIGKV and SLIGRL result in different effects on β-arrestin recruitment. 2f-LIGRLO and GB110 are equipotent and have higher potencies than SLIGKV and SLIGRL which also are equipotent. PAR2-PK plasmids were successfully constructed and suitable for use in the DiscoverX β-arrestin recruitment assay. PAR2-PK plasmids were successfully transfected to the 1321N1 β-arrestin-EA cell line. PAR2 was expressed and functional on the membrane shown by the FLIPR assay. PAR2-PK was functional in the β-arrestin recruitment study. Data suggests the importance of residues E232, Y323, Y326 and D228 of PAR2 for β-arrestin-mediated signalling induced by agonists SLIGKV, SLIGRL, 2f-LIGRLO and GB110 (except E232). Data also suggest that the suggested orthogonal site in the published crystal structure is the orthogonal binding site in β-arrestin recruitment for agonist SLIGKV, SLIGRL, GB110 and 2f-LIGLRO.

References

AAT BIOQUEST. 2017. *Screen Quest™ Fluo-8 No Wash Calcium Assay Kit* [Online]. Available: http://www.aatbio.com/products/screen-quest-fluo-8-no-wash-calcium-assay-kit [Accessed 2017-10-19].

ALBERTS, B., JOHNSON, A., LEWIS, J., RAFF, M., ROBERTS, K. & WALTER, P. 2008. *Molecular Biology of the Cell*, Garland Science.

ATTRILL, H., HARDING, P. J., SMITH, E., ROSS, S. & WATTS, A. 2009. Improved yield of a ligand-binding GPCR expressed in E. coli for structural studies. *Protein Expression and Purification,* 64**,** 32-38.

AYOUB, M. A. & PIN, J.-P. 2013. Interaction of Protease-Activated Receptor 2 with G Proteins and β-Arrestin 1 Studied by Bioluminescence Resonance Energy Transfer. *Frontiers in Endocrinology,* 4**,** 196.

BADEANLOU, L., FURLAN-FREGUIA, C., YANG, G., RUF, W. & SAMAD, F. 2011. Tissue factor-PAR2 signaling promotes diet-induced obesity and adipose inflammation. *Nature medicine,* 17**,** 1490-1497.

BOCHKOV, Y. A. & PALMENBERG, A. C. 2006. Translational efficiency of EMCV IRES in bicistronic vectors is dependent upon IRES sequence and gene location. *Biotechniques,* 41**,** 283.

BRISSON, M., HE, Y., LI, S., YANG, J. P. & HUANG, L. 1999. A novel T7 RNA polymerase autogene for efficient cytoplasmic expression of target genes. *Gene Therapy,* 6**,** 263.

CHEN, X., ZARO, J. & SHEN, W.-C. 2013. Fusion Protein Linkers: Property, Design and Functionality. *Advanced drug delivery reviews,* 65**,** 1357-1369.

CHENG, R. K. Y., FIEZ-VANDAL, C., SCHLENKER, O., EDMAN, K., AGGELER, B., BROWN, D. G., BROWN, G. A., COOKE, R. M., DUMELIN, C. E., DORE, A. S., GESCHWINDNER, S., GREBNER, C., HERMANSSON, N. O., JAZAYERI, A., JOHANSSON, P., LEONG, L., PRIHANDOKO, R., RAPPAS, M., SOUTTER, H., SNIJDER, A., SUNDSTROM, L., TEHAN, B., THORNTON, P., TROAST, D., WIGGIN, G., ZHUKOV, A., MARSHALL, F. H. & DEKKER, N. 2017. Structural insight into allosteric modulation of protease-activated receptor 2. *Nature,* 545**,** 112-115.

DEFEA, K. A., ZALEVSKY, J., THOMA, M. S., DÉRY, O., MULLINS, R. D. & BUNNETT, N. W. 2000. β-Arrestin–Dependent Endocytosis of Proteinase-Activated Receptor 2 Is Required for Intracellular Targeting of Activated Erk1/2. *The Journal of Cell Biology,* 148**,** 1267-1282.

DISCOVERX. 2017. *[User Manual] PathHunter® β-Arrestin Assay for GPCR Cell Lines* [Online]. Available: https://www.discoverx.com/tools-resources/document-resource-library/documents/user-manual-pathhunter-%CE%B2-arrestin-assay-for-gpcr-c [Accessed 2017-09-19].

EINHAUER, A. & JUNGBAUER, A. 2001. The FLAG™ peptide, a versatile fusion tag for the purification of recombinant proteins. *Journal of Biochemical and Biophysical Methods,* 49**,** 455-465.

FREDRIKSSON, R., LAGERSTRÖM, M. C., LUNDIN, L.-G. & SCHIÖTH, H. B. 2003. The G-Protein-Coupled Receptors in the Human Genome Form Five Main Families. Phylogenetic Analysis, Paralogon Groups, and Fingerprints. *Molecular Pharmacology,* 63**,** 1256-1272.

GE, L., SHENOY, S. K., LEFKOWITZ, R. J. & DEFEA, K. 2004. Constitutive protease-activated receptor-2-mediated migration of MDA MB-231 breast cancer cells requires both β-arrestin-1 and-2. *Journal of Biological Chemistry,* 279**,** 55419-55424.

GESZTELYI, R., ZSUGA, J., KEMENY-BEKE, A., VARGA, B., JUHASZ, B. & TOSAKI, A. 2012. The Hill equation and the origin of quantitative pharmacology. *Archive for History of Exact Sciences,* 66**,** 427-438.

GIBSON, D. G., YOUNG, L., CHUANG, R.-Y., VENTER, J. C., HUTCHISON, C. A. & SMITH, H. O. 2009. Enzymatic assembly of DNA molecules up to several hundred kilobases. *Nat Meth,* 6**,** 343-345.

GOLAN, D. E. 2011. *Principles of pharmacology : the pathophysiologic basis of drug therapy,* Philadelphia, Pa.; London, Lippincott Williams & Wilkins.

GRAPHPAD. 2016. *Equation: log(agonist) vs. response -- Variable slope* [Online]. Available: http://www.graphpad.com/guides/prism/7/curve-fitting/reg_dr_stim_variable.htm?toc=0&printWindow [Accessed 2017-10-31].

GRAPHPAD. 2017. *Why does Prism report the standard error for logEC50, but not for the EC50 itself, when it fits dose-response curves?* [Online]. Available: http://www.graphpad.com/support/faqid/34/ [Accessed 2017-11-21].

GRAPHPAD. 2018. *How should I compute an "average" EC50 for several experiments? How can I express its uncertainty or standard deviation?* [Online]. Available: https://www.graphpad.com/support/faq/how-should-i-compute-an-average-ec50-for-several-experiments-how-can-i-express-its-uncertainty-or-standard-deviation/ [Accessed 2018-05-08].

HERSHFIELD, V., BOYER, H. W., YANOFSKY, C., LOVETT, M. A. & HELINSKI, D. R. 1974. Plasmid ColE1 as a Molecular Vehicle for Cloning and Amplification of DNA. *Proceedings of the National Academy of Sciences of the United States of America,* 71**,** 3455-3459.

HONEGGER, B. K., MOCIKAT, R. & PLIICKTHUN, A. 1997. Specific detection of his-tagged proteins with recombinant anti-His tag scFv-phosphatase or scFv-phage fusions. *Biotechniques,* 22**,** 140-149.

KANKE, T., KABEYA, M., KUBO, S., KONDO, S., YASUOKA, K., TAGASHIRA, J., ISHIWATA, H., SAKA, M., FURUYAMA, T., NISHIYAMA, T., DOI, T., HATTORI, Y., KAWABATA, A., CUNNINGHAM, M. R. & PLEVIN, R. 2009. Novel antagonists for proteinase-activated receptor 2: inhibition of cellular and vascular responses in vitro and in vivo. *British Journal of Pharmacology,* 158**,** 361-371.

KOZAK, M. 1986. Point mutations define a sequence flanking the AUG initiator codon that modulates translation by eukaryotic ribosomes. *Cell,* 44**,** 283-292.

LEARY, J. J., BRIGATI, D. J. & WARD, D. C. 1983. Rapid and sensitive colorimetric method for visualizing biotin-labeled DNA probes hybridized to DNA or RNA immobilized on nitrocellulose: Bio-blots. *Proceedings of the National Academy of Sciences of the United States of America,* 80**,** 4045-4049.

MACINTYRE, E. H., PONTÉN, J. & VATTER, A. 1972. The ultrastructure of human and murine astrocytes and of human fibroblasts in culture. *APMIS,* 80**,** 267-283.

MAHMOOD, T. & YANG, P.-C. 2012. Western Blot: Technique, Theory, and Trouble Shooting. *North American Journal of Medical Sciences,* 4**,** 429-434.

MATHEWS, C. K., VAN HOLDE, K. E., APPLING, D. R. & ANTHONY-CAHILL, S. J. 2012. *Biochemistry*, Pearson.

MAXCYTE INC. 2017. *MaxCyte STX®* [Online]. Available: http://www.maxcyte.com/products-services/stx/ [Accessed 2017-12-29].

MOYA, P. R., BERG, K. A., GUTIÉRREZ-HERNANDEZ, M. A., SÁEZ-BRIONES, P., REYES-PARADA, M., CASSELS, B. K. & CLARKE, W. P. 2007. Functional Selectivity of Hallucinogenic Phenethylamine and Phenylisopropylamine Derivatives at Human 5-Hydroxytryptamine (5-HT)2A and 5-HT2C receptors. *Journal of Pharmacology and Experimental Therapeutics,* 321**,** 1054.

NAGELE, P. 2003. Misuse of standard error of the mean (sem) when reporting variability of a sample. A critical evaluation of four anaesthesia journals. *BJA: British Journal of Anaesthesia,* 90**,** 514-516.

NEUBIG, R. R., SPEDDING, M., KENAKIN, T. & CHRISTOPOULOS, A. 2003. International Union of Pharmacology Committee on Receptor Nomenclature and Drug Classification. XXXVIII. Update on Terms and Symbols in Quantitative Pharmacology. *Pharmacological Reviews,* 55**,** 597-606.

NIFOROU, K. N., ANAGNOSTOPOULOS, A. K., VOUGAS, K., KITTAS, C., GORGOULIS, V. G. & TSANGARIS, G. T. 2008. The proteome profile of the human osteosarcoma U2OS cell line. *Cancer Genomics-Proteomics,* 5**,** 63-77.

NOORBAKHSH, F., TSUTSUI, S., VERGNOLLE, N., BOVEN, L. A., SHARIAT, N., VODJGANI, M., WARREN, K. G., ANDRADE-GORDON, P., HOLLENBERG, M. D. & POWER, C. 2006. Proteinase-activated receptor 2 modulates neuroinflammation in experimental autoimmune encephalomyelitis and multiple sclerosis. *The Journal of Experimental Medicine,* 203**,** 425-435.

POTTER, H. & HELLER, R. 2003. Transfection by Electroporation. *Current protocols in molecular biology / edited by Frederick M. Ausubel ... [et al.],* CHAPTER**,** Unit-9.3.

PRINZ, H. 2010. Hill coefficients, dose–response curves and allosteric mechanisms. *Journal of Chemical Biology,* 3**,** 37-44.

RAJAGOPAL, S., RAJAGOPAL, K. & LEFKOWITZ, R. J. 2010. Teaching old receptors new tricks: biasing seven-transmembrane receptors. *Nat Rev Drug Discov,* 9**,** 373-86.

RAMACHANDRAN, R., MIHARA, K., CHUNG, H., RENAUX, B., LAU, C. S., MURUVE, D. A., DEFEA, K. A., BOUVIER, M. & HOLLENBERG, M. D. 2011. Neutrophil elastase acts as a biased agonist for proteinase-activated receptor-2 (PAR2). *Journal of Biological Chemistry,* 286**,** 24638-24648.

SANGER, F., NICKLEN, S. & COULSON, A. R. 1977. DNA sequencing with chain-terminating inhibitors. *Proceedings of the National Academy of Sciences of the United States of America,* 74**,** 5463-5467.

SCARSELLI, M. & DONALDSON, J. G. 2009. Constitutive Internalization of G Protein-coupled Receptors and G Proteins via Clathrin-independent Endocytosis. *The Journal of Biological Chemistry,* 284**,** 3577-3585.

SCHROEDER, K. S. & NEAGLE, B. D. 1996. FLIPR: A New Instrument for Accurate, High Throughput Optical Screening. *Journal of Biomolecular Screening,* 1**,** 75-80.

SHUKLA, A. K., WESTFIELD, G. H., XIAO, K., REIS, R. I., HUANG, L. Y., TRIPATHI-SHUKLA, P., QIAN, J., LI, S., BLANC, A., OLESKIE, A. N., DOSEY, A. M., SU, M., LIANG, C. R., GU, L. L., SHAN, J. M., CHEN, X., HANNA, R., CHOI, M., YAO, X. J., KLINK, B. U., KAHSAI, A. W., SIDHU, S. S., KOIDE, S., PENCZEK, P. A., KOSSIAKOFF, A. A., JR, V. L. W., KOBILKA, B. K., SKINIOTIS, G. & LEFKOWITZ, R. J. 2014. Visualization of arrestin recruitment by a G-protein-coupled receptor. *Nature,* 512**,** 218-222.

SMRCKA, A. V. 2008. G protein βγ subunits: Central mediators of G protein-coupled receptor signaling. *Cellular and molecular life sciences : CMLS,* 65**,** 2191-2214.

SRIRAM, K. & INSEL, P. A. 2018. GPCRs as targets for approved drugs: How many targets and how many drugs? *Molecular Pharmacology*.

SUEN, J. Y., ADAMS, M. N., LIM, J., MADALA, P. K., XU, W., COTTERELL, A. J., HE, Y., YAU, M. K., HOOPER, J. D. & FAIRLIE, D. P. 2017. Mapping transmembrane residues of proteinase activated receptor 2 (PAR2) that influence ligand-modulated calcium signaling. *Pharmacological Research,* 117**,** 328-342.

SUEN, J. Y., BARRY, G. D., LOHMAN, R. J., HALILI, M. A., COTTERELL, A. J., LE, G. T. & FAIRLIE, D. P. 2012. Modulating human proteinase activated receptor 2 with a novel antagonist (GB88) and agonist (GB110). *British Journal of Pharmacology,* 165**,** 1413-1423.

THE HUMAN PROTEIN ATLAS. *F2RL1* [Online]. The Human Protein Atlas. Available: http://www.proteinatlas.org/ENSG00000164251-F2RL1/tissue [Accessed 2017-09-18].

TOMOMORI-SATO, C., SATO, S., CONAWAY, R. C. & CONAWAY, J. W. 2013. Immunoaffinity Purification of Protein Complexes from Mammalian Cells. *Methods in molecular biology (Clifton, N.J.),* 977**,** 273-287.

UUSITALO-JARVINEN, H., KUROKAWA, T., MUELLER, B. M., ANDRADE-GORDON, P., FRIEDLANDER, M. & RUF, W. 2007. Role of Protease Activated Receptor 1 and 2 Signaling in Hypoxia-Induced Angiogenesis. *Arteriosclerosis, Thrombosis, and Vascular Biology,* 27**,** 1456.

VENKATAKRISHNAN, A. J., DEUPI, X., LEBON, G., TATE, C. G., SCHERTLER, G. F. & BABU, M. M. 2013. Molecular signatures of G-protein-coupled receptors. *Nature,* 494**,** 185-194.

VERSTEEG, H. H., SCHAFFNER, F., KERVER, M., ELLIES, L. G., PATRICIA, A.-G., MUELLER, B. M. & RUF, W. 2008. Protease activated receptor (PAR) 2, but not PAR1 signaling promotes the development of mammary adenocarcinoma in PyMT mice. *Cancer research,* 68**,** 7219-7227.

WISLER, J. W., DEWIRE, S. M., WHALEN, E. J., VIOLIN, J. D., DRAKE, M. T., AHN, S., SHENOY, S. K. & LEFKOWITZ, R. J. 2007. A unique mechanism of β-blocker action: Carvedilol stimulates β-arrestin signaling. *Proceedings of the National Academy of Sciences,* 104**,** 16657-16662.

WITHEROW, D. S., GARRISON, T. R., MILLER, W. E. & LEFKOWITZ, R. J. 2004. β-Arrestin inhibits NF-κB activity by means of its interaction with the NF-κB inhibitor IκBα. *Proceedings of the National Academy of Sciences of the United States of America,* 101**,** 8603-8607.

YAU, M. K., LIU, L. & FAIRLIE, D. P. 2013. Toward drugs for protease-activated receptor 2 (PAR2). *J Med Chem,* 56**,** 7477-97.

ZHANG, Y., KOWAL, D., KRAMER, A. & DUNLOP, J. 2003. Evaluation of FLIPR Calcium 3 Assay Kit—A New No-Wash Fluorescence Calcium Indicator Reagent. *Journal of Biomolecular Screening,* 8**,** 571-577.

ZHAO, P., LIEU, T., BARLOW, N., METCALF, M., VELDHUIS, N. A., JENSEN, D. D., KOCAN, M., SOSTEGNI, S., HAERTEIS, S., BARAZNENOK, V., HENDERSON, I., LINDSTRÖM, E., GUERRERO-ALBA, R., VALDEZ-MORALES, E. E., LIEDTKE, W., MCINTYRE, P., VANNER, S. J., KORBMACHER, C. & BUNNETT, N. W. 2014a. Cathepsin S Causes Inflammatory Pain via Biased Agonism of PAR(2) and TRPV4. *The Journal of Biological Chemistry,* 289**,** 27215-27234.

ZHAO, P., METCALF, M. & BUNNETT, N. W. 2014b. Biased signaling of protease-activated receptors. *Front Endocrinol (Lausanne),* 5**,** 67.

ZOUDILOVA, M., MIN, J., RICHARDS, H. L., CARTER, D., HUANG, T. & DEFEA, K. A. 2010. β-Arrestins scaffold cofilin with chronophin to direct localized actin filament severing and membrane protrusions downstream of protease-activated receptor-2. *Journal of Biological Chemistry,* 285**,** 14318-14329.

Appendix A PAR2 amino acid sequence

Colors:
Blue: N-terminus
Green: Transmembrane domains 1-7
Red: Intracellular Loops 1-3
Orange: Extracellular Loops 1-3
Purple: Helix 8 (beginning of C-terminus)
Light blue: N-terminus without Helix 8

```
1   MRSPSAAWLLGAAILLAASLSCSGTIQGTNRSSKGRSLIGKVDGTSHVTGKGVTVETVFS
61  VDEFSASVLTGKLTTVFLPIVYTIVFVVGLPSNGMALWVFLFRTKKKHPAVIYMANLALA
121 DLLSVIWFPLKIAYHIHGNNWIYGEALCNVLIGFFYGNMYCSILFMTCLSVQRYWVIVNP
181 MGHSRKKANIAIGISLAIWLLILLVTIPLYVVKQTIFIPALNITTCHDVLPEQLLVGDMF
241 NYFLSLAIGVFLFPAFLTASAYVLMIRMLRSSAMDENSEKKRKRAIKLIVTVLAMYLICF
301 TPSNLLLVVHYFLIKSQGQSHVYALYIVALCLSTLNSCIDPFVYYFVSHDFRDHAKNALL
361 CRSVRTVKQMQVSLTSKKHSRKSSSYSSSSTTVKTSY
```

Based on (Yau et al., 2013).

Appendix B Structural formulas of agonists

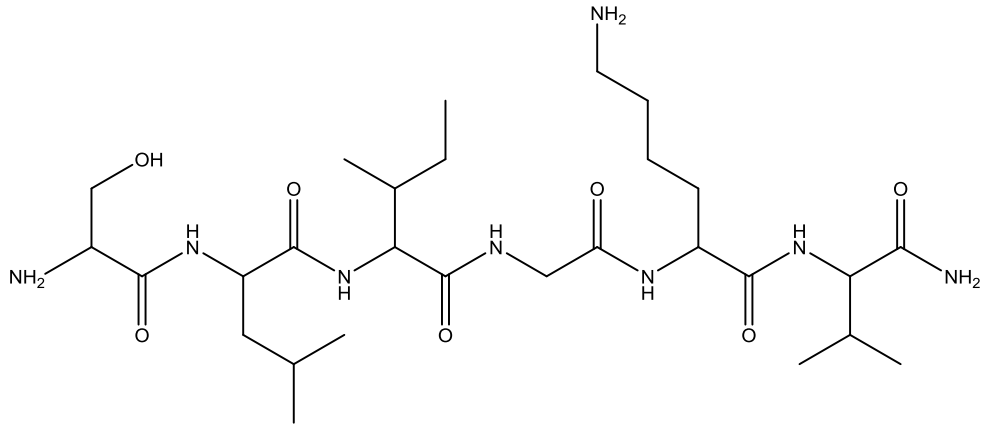

A) H_2N-SLIGKV

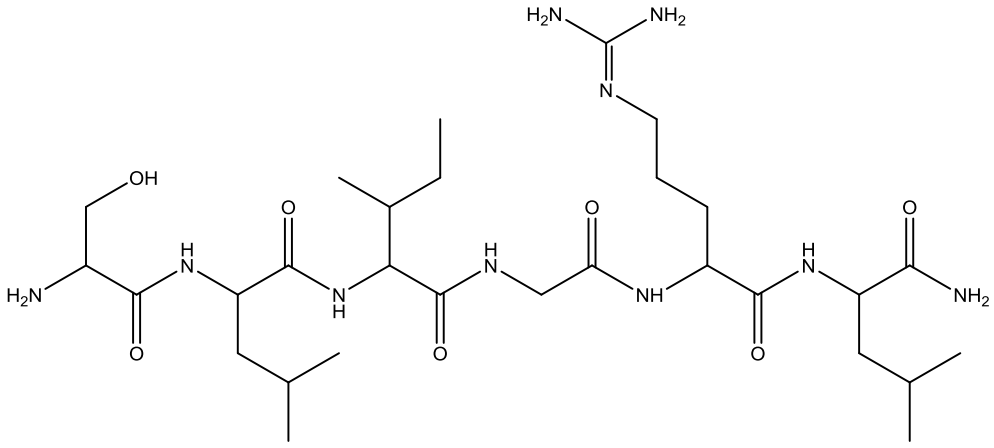

B) H_2N-SLIGRL

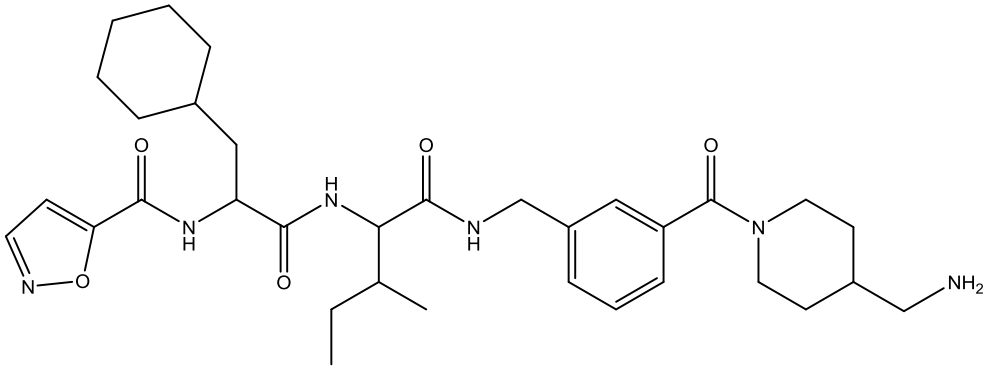

C) GB110

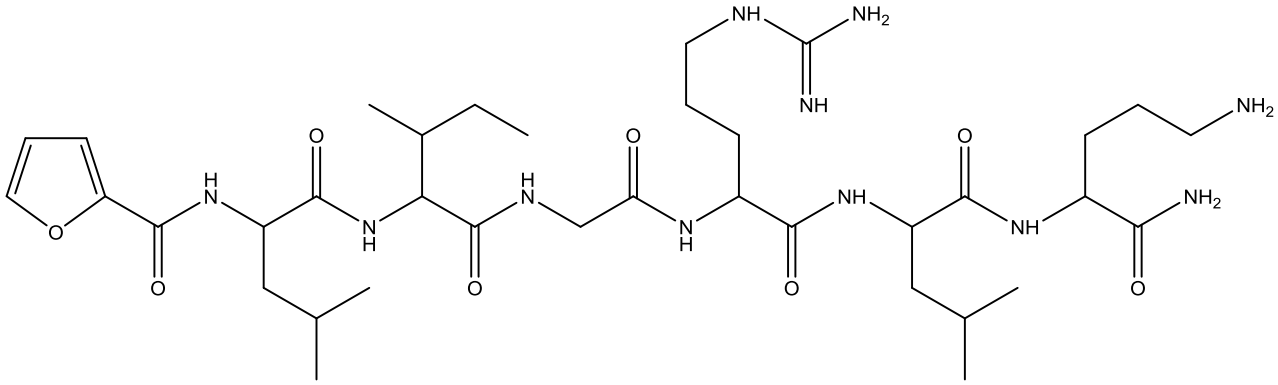

D) 2f-LIGRLO

Figure 24. Structural formulas of agonists A) H_2N-SLIGKV, B) H_2N-SLIGRL, C) GB110 and D) 2f-LIGRLO

Appendix C Amino acids

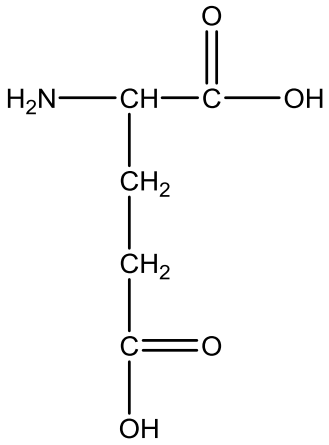

A) Glutamic Acid (E)

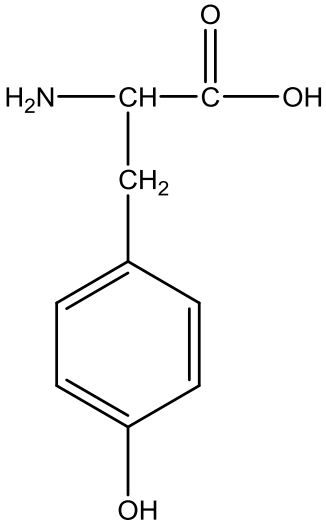

B) Tyrosine (Y)

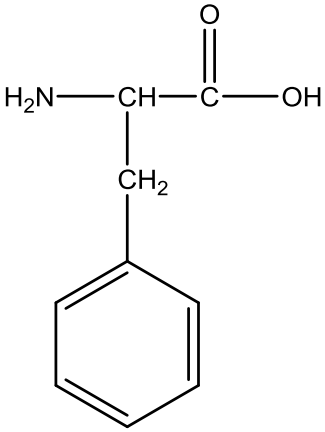

C) Phenylalanine (F)

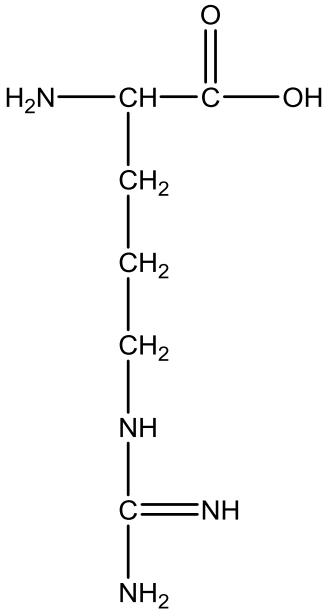

D) Arginine (R)

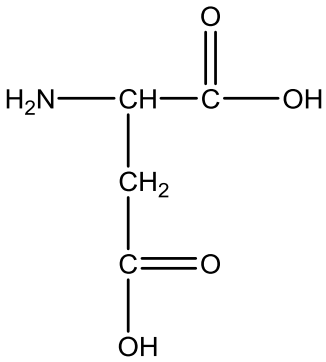

E) Aspartic Acid (D)

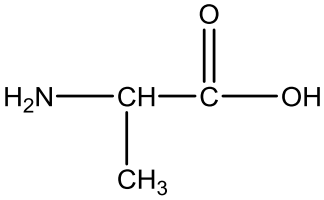

F) Alanine (A)

Figure 25. Amino acids glutamic acid (E), tyrosine (Y), phenylalanine (F), arginine (R), aspartic Acid (D) and alanine (A) which is in focus during this project.

Appendix D Plasmids

Appendix D1 PK-plasmid

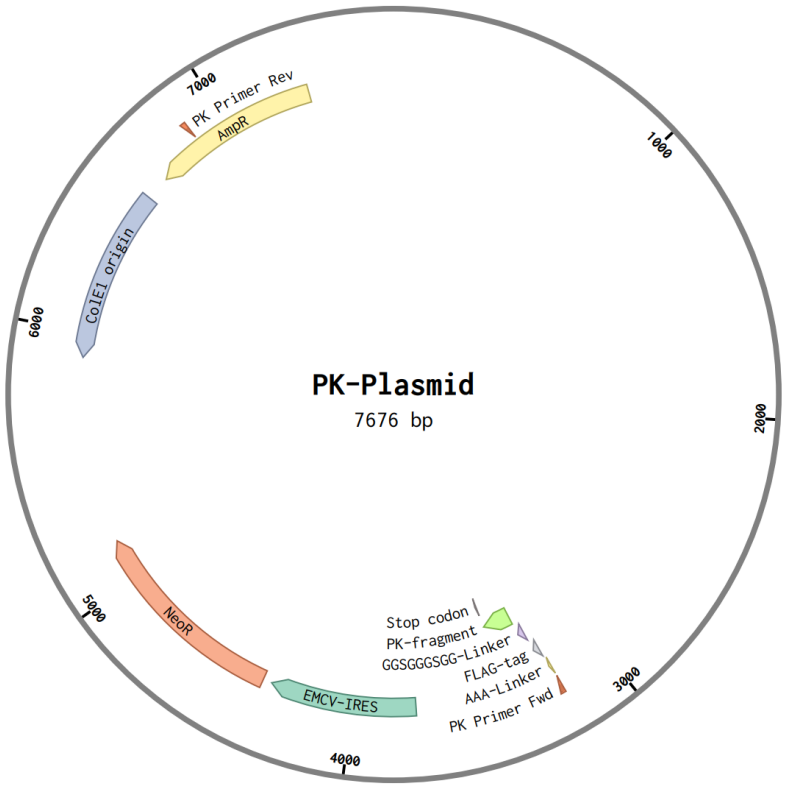

Figure 26. PK-Plasmid with PK-fragment, EMCV-IRES, FLAG-tag, GGSGGGSGG-linker, AAA-linker, ColE1 origin of replication and neomycin and ampicillin resistance genes. Figured annotated in and obtained from Benchling.

Appendix D2 PAR2 His Plasmid

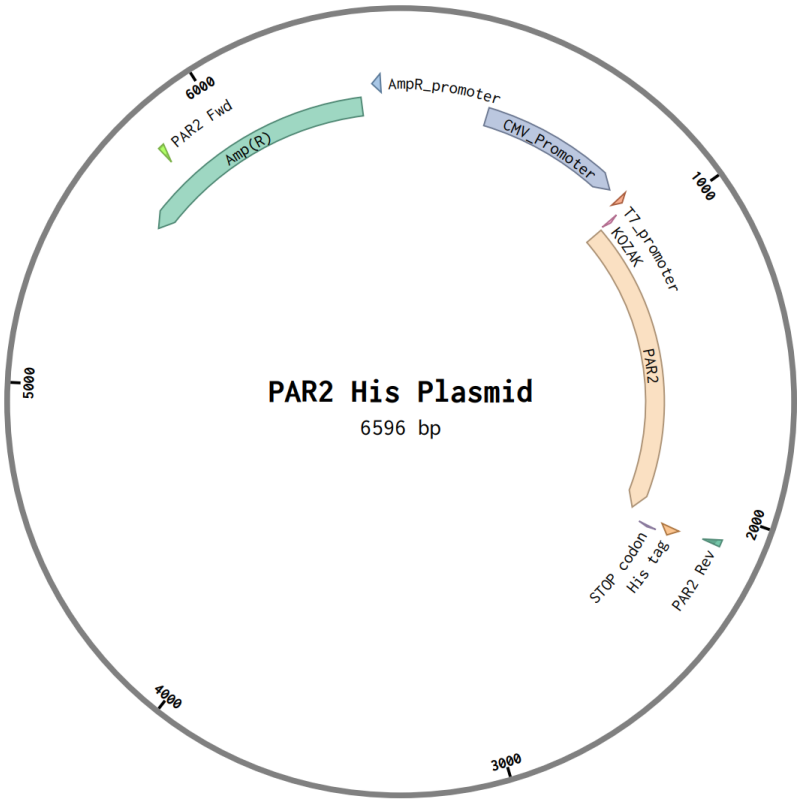

Figure 27. PAR2 His plasmid with CMV and T7 promoter together with a Kozak sequence prior PAR2 gene, ampicillin resistance gene, His tag and stop codon. Figured annotated in and obtained from Benchling.

Appendix D3 PAR2 (V5)-PK Plasmid Assembly

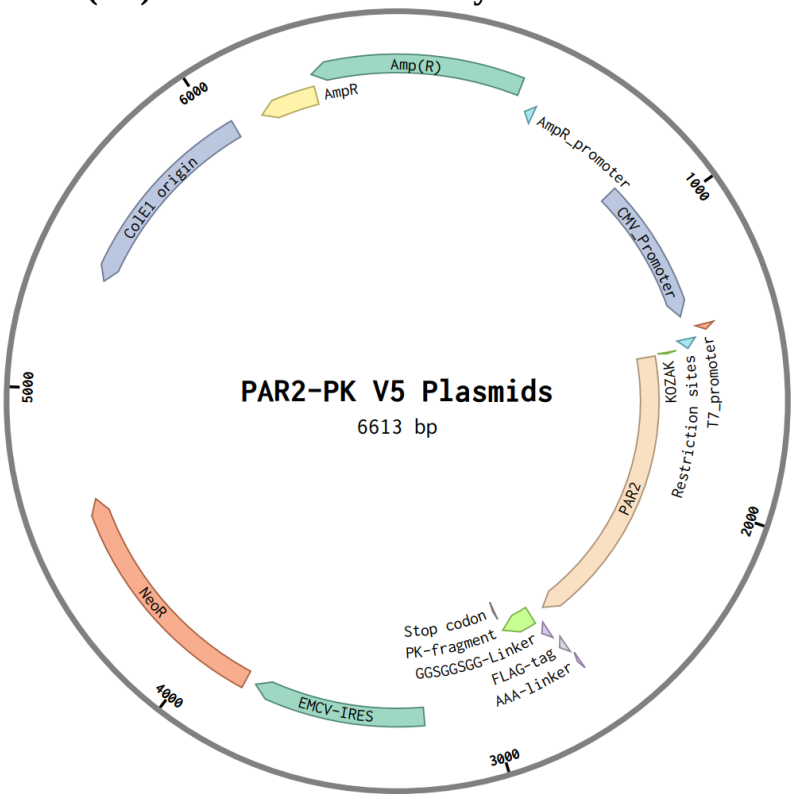

Figure 28. PAR2 (V5)-PK plasmid from Gibson assembly using fragments from PAR2 V5 plasmid and PK-Plasmid to obtain PAR2 (V5)-PK plasmids. Plasmid consists of a CMV and T7 promoter together with a Kozak sequence prior PAR2 gene, PK-fragment, EMCV-IRES, FLAG-tag, GGSGGGSGG-linker, AAA-linker, stop codon, ColE1 origin of replication and neomycin and ampicillin resistance genes. Figured annotated in and obtained from Benchling.

Appendix E Example Calculations

SLIGKV/SLIGRL @ 50 mM

stock	5.00E-02										
total volume needed (ul)	40	30									
Volume of stock (ul)		19.2									
Volume of previous conc (ul)			10.0	3	3	3	3	3	3	3	3
Volume of buffer (ul)		20.8	20.0	27	27	27	27	27	27	27	27
Prep Plate 80x	16	2.40E-02	8.00E-03	2.40E-03	8.00E-04	2.40E-04	8.00E-05	2.40E-05	8.00E-06	2.40E-06	8.00E-07
		5 ul from Prep plate + 75 ul DMEM media to get agonist plate (triplicates)									
Agonist plate 5x	5	1.50E-03	5.00E-04	1.50E-04	5.00E-05	1.50E-05	5.00E-06	1.50E-06	5.00E-07	1.50E-07	5.00E-08
		5 ul of Agonist plate into 20 ul of cells to get Final Assay Concentration (FAC)/FLIPR 10µl to 40 µl Buffer									
FAC		3.00E-04	1.00E-04	3.00E-05	1.00E-05	3.00E-06	1.00E-06	3.00E-07	1.00E-07	3.00E-08	1.00E-08

acetylated GB110 and 2f-LIGRLO

stock	**5.00E-03**									
total volume needed (ul)	40	30								
Volume of stock (ul)		6.4								
Volume of previous conc (ul)			9.0	3	3	3	3	3	3	3
Volume of buffer (ul)		33.6	21.0	27	27	27	27	27	27	27

Prep Plate 80x	16	8.00E-04	2.40E-04	8.00E-05	2.40E-05	8.00E-06	2.40E-06	8.00E-07	2.40E-07	8.00E-08	2.40E-08

5 ul from Prep plate + 75 ul DMEM media to get agonist plate (triplicates)

Agonist plate 5x	5	5.00E-05	1.50E-05	5.00E-06	1.50E-06	5.00E-07	1.50E-07	5.00E-08	1.50E-08	5.00E-09	1.50E-09

5 ul of Agonist plate into 20 ul of cells to get Final Assay Concentration (FAC)/FLIPR 10µl to 40 µl Buffer

FAC		1.00E-05	3.00E-06	1.00E-06	3.00E-07	1.00E-07	3.00E-08	1.00E-08	3.00E-09	1.00E-09	3.00E-10

Controls	**DMSO**		**Water**	**Bf**
	stock	1.00E-02		
Volume of stock (ul)	6.4		19.2	
Volume of previous conc (ul)				
Volume of buffer (ul)	33.6		20.8	40

Appendix F Primer Sequences

Appendix F1PCR primers

Table 11. PCR primers used in this study where uppercase characters hybridize to the template and lowercase characters shows the overlapping overhang.

Primer	Sequence (5´→3´)
PK Forward	ccaccgtgaaaaccagctacGCAGCAGCAGATTACAAGGA
PK Reverse	ggaccacttctgcgctcggcCCTTCCGGCTGGCTGGTTTA
PAR2 Forward	taaaccagccagccggaaggGCCGAGCGCAGAAGTGGTCC
PAR2 Reverse	tccttgtaatctgctgctgcGTAGCTGGTTTTCACGGTGGTG

Appendix F2Sequencing primers

Table 12. Sequencing primers for PAR2 His and V5 Gibson assemblies.

Primer	Sequence (5´→3´)
PAR2 His	TGAGCACCCTGAACAGC
PAR2 V5	TGAGCACCCTGAATAGC

Appendix G Thermocycling conditions

Table 13. 55-65°C Gradient PCR protocol.

Step	Temp	Time
Initial Denaturation	98°C	30 seconds
30 cycles	98°C	10 seconds
	Gradient 55-65°C	25 seconds
	72 °C	150 seconds
Final extension	72 °C	5 min
Hold	4-10 °C	-

Table 14. 2-step PCR protocol

Step	Temp	Time
Initial Denaturation	98°C	30 seconds
30 cycles	98°C	10 seconds
	72°C	150 seconds
Final extension	72°C	5 min
Hold	4°C	-

Appendix H ScaI restriction digestions

Appendix H1.1 WT (V5)-PK, Y326A-PK, WT (His)-PK and D228A-PK

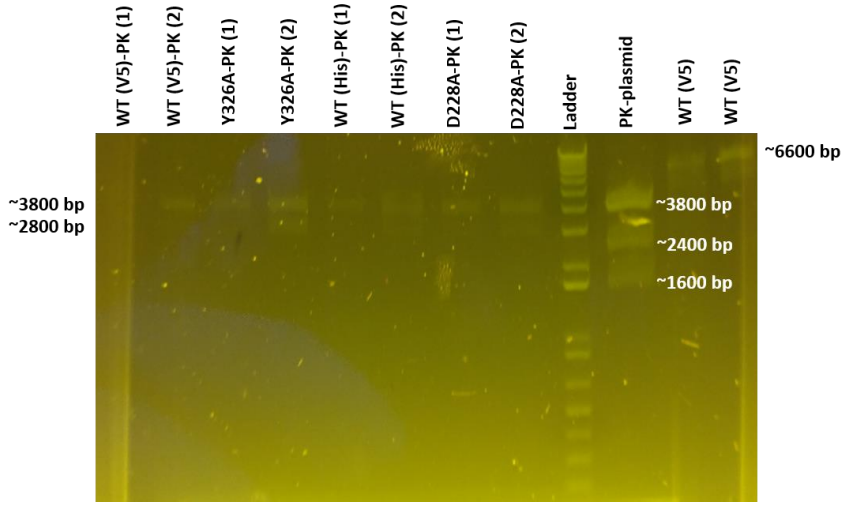

Figure 29. Gel of ScaI digestions for WT (V5)-PK, Y326A-PK, WT (His)-PK, D228A-PK, WT (His) control, WT (V5) control and PK-plasmid control. E-Gel 1 Kb Plus DNA ladder also visualized. Expected bands of PAR2 (His)-PK plasmids (3761 bp and 2818bp), PAR2 (V5)-PK plasmids (3761 bp and 2852 bp), PK-plasmid control (3761 bp, 2351 bp and 1564bp), PAR2 WT (V5) (6639 bp) and PAR2 WT (His) (6596 bp)

Appendix H1.2 Y82F-PK, D228A-PK and E232R-PK

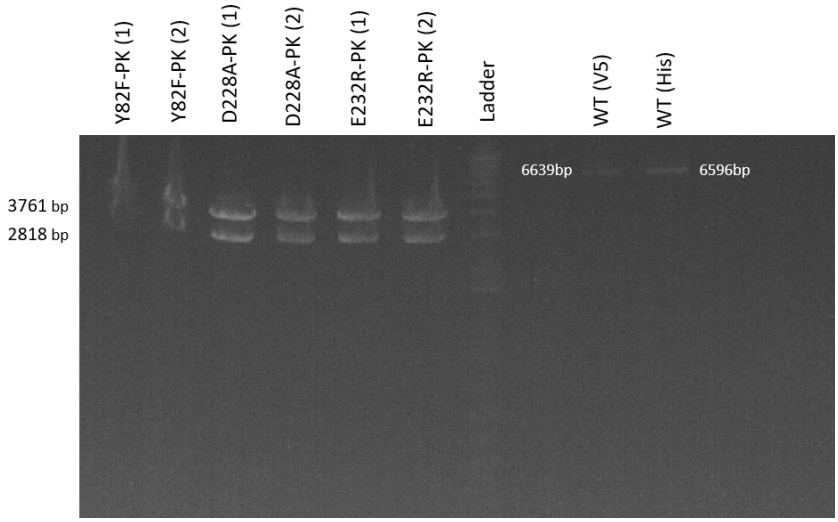

Figure 30. Gel of ScaI digestions for Y82F-PK (1,2), D228A-PK (1,2), E232R-PK (1,2), PAR2 WT (His) control and PAR2 WT (V5) control. E-Gel 1 Kb Plus DNA ladder also visualized. Expected bands of PAR2 (His)-PK plasmids (3761 and 2818 bp), PK-plasmid control (3761, 2351 and 1564 bp), PAR2 (V5) WT (6639 bp) and PAR2 WT (His) (6596 bp).

Appendix I FLIPR Potency data

Tables 15A-L. EC_{50}, pEC_{50}±SEM and E_{max}±SEM for agonists SLIGKV, SLIGRL, GB110 and 2f-LIGRLO in FLIPR based on mean values of two experimental replicates each consisting of biological triplicate measurements except for E232R-PK and E232R*-PK where one experimental replicate was done. Data represented in tables: A) 1321N1 β-arrestin-EA cells control, B) U2OS PAR2-PK/β-arrestin-EA cells control, transiently transfected 1321N1 β-arrestin-EA cells with C) WT (V5)-PK, D) E232A-PK, E) Y323F-PK, F) Y326A-PK, G) Y323A-PK, H) WT (His)-PK, I) Y82F-PK, J) D228A-PK and K) E232R*-PK and L) E232R-PK. N.R indicates no response.

A) 1321N1 β-arrestin-EA Control

Agonist	EC_{50}	pEC_{50} ± SEM	E_{max} ± SEM
SLIGKV	N. R	N. R	N. R
SLIGRL	N. R	N. R	N. R
GB110	N. R	N. R	N. R
2f-LIGRLO	N. R	N. R	N. R

B) U2OS PAR2-PK/β-arrestin-EA Control

Agonist	EC_{50}	pEC_{50} ± SEM	E_{max} ± SEM
SLIGKV	2.34E-7	6.67 ± 0.063	702.42 ± 84.12
SLIGRL	1.28E-7	6.93 ± 0.077	896.57 ± 102.70
GB110	2.69E-8	8.20 ± 0.276	711.91 ± 53.05
2f-LIGRLO	3.38E-8	7.54 ± 0.105	625.96 ± 51.88

C) 1321N1 WT (V5)-PK/β-arrestin-EA

Agonist	EC_{50}	pEC_{50} ± SEM	E_{max} ± SEM
SLIGKV	3.75E-6	5.61 ± 0.114	380.26 ± 41.42
SLIGRL	1.43E-6	5.95 ± 0.092	367.70 ± 48.85
GB110	3.19E-7	6.55 ± 0.061	403.39 ± 41.97
2f-LIGRLO	2.32E-7	6.67 ± 0.053	380.34 ± 42.60

D) 1321N1 E232A-PK/β-arrestin-EA

Agonist	EC_{50}	pEC_{50} ± SEM	E_{max} ± SEM
SLIGKV	1.93E-5	4.83 ± 0.138	410.37 ± 69.91
SLIGRL	5.93E-6	5.40 ± 0.178	477.94 ± 65.26
GB110	4.43E-7	6.43 ± 0.122	515.59 ± 44.88
2f-LIGRLO	1.18E-6	6.26 ± 0.21	448.41 ± 54.59

E) 1321N1 Y323F-PK/β-arrestin-EA

Agonist	EC_{50}	pEC_{50} ± SEM	E_{max} ± SEM
SLIGKV	5.89E-5	4.24 ± 0.04	251.63 ± 17.84
SLIGRL	2.12E-5	4.71 ± 0.769	361.85 ± 31.83
GB110	1.58E-6	5.81 ± 0.049	277.93 ± 14.57
2f-LIGRLO	9.64E-7	6.02 ± 0.016	373.37 ± 14.89

F) 1321N1 Y326A-PK/β-arrestin-EA

Agonist	EC_{50}	pEC_{50} ± SEM	E_{max} ± SEM
SLIGKV	4.49E-4	3.36 ± 0.038	119.88 ± 18.33
SLIGRL	1.41E-4	3.90 ± 0.089	286.91 ± 57.30
GB110	2.64E-6	5.64 ± 0.093	362.84 ± 43.18
2f-LIGRLO	3.51E-6	5.60 ± 0.153	309.57 ± 54.91

G) 1321N1 Y323A-PK/β-arrestin-EA

Agonist	EC_{50}	pEC_{50} ± SEM	E_{max} ± SEM
SLIGKV	N. R	N. R	N. R
SLIGRL	N. R	N. R	N. R
GB110	N. R	N. R	N. R
2f-LIGRLO	N. R	N. R	N. R

H) 1321N1 WT (His)-PK/β-arrestin-EA

Agonist	EC_{50}	pEC_{50} ± SEM	E_{max} ± SEM
SLIGKV	1.03E-5	5.05 ± 0.109	375.04 ± 78.05
SLIGRL	3.49E-6	5.47 ± 0.052	389.15 ± 68.85
GB110	7.58E-7	6.15 ± 0.073	321.82 ± 65.35
2f-LIGRLO	3.69E-7	6.44 ± 0.029	336.78 ± 59.59

I) 1321N1 Y82F-PK/β-arrestin-EA

Agonist	EC_{50}	pEC_{50} ± SEM	E_{max} ± SEM
SLIGKV	1.42E-5	4.86 ± 0.064	340.06 ± 29.87
SLIGRL	5.84E-6	5.26 ± 0.064	335.16 ± 33.97
GB110	1.07E-6	5.98 ± 0.031	239.88 ± 35.03
2f-LIGRLO	1.39E-6	6.06 ± 0.167	264.07 ± 30.88

J) 1321N1 D228A-PK/β-arrestin-EA

Agonist	EC_{50}	pEC_{50} ± SEM	E_{max} ± SEM
SLIGKV	N. R	N. R	N. R
SLIGRL	1.43E-3	3.00 ± 0.162	105.70 ± 22.28
GB110	N. R	N. R	N. R
2f-LIGRLO	2.22E-5	4.71 ± 0.072	92 ± 20.07

K) 1321N1 E232R*-PK/β-arrestin-EA

Agonist	EC_{50}	pEC_{50} ± SEM	E_{max} ± SEM
SLIGKV	N. R	N. R	N. R
SLIGRL	N. R	N. R	N. R
GB110	N. R	N. R	N. R
2f-LIGRLO	N. R	N. R	N. R

L) 1321N1 E232R-PK/β-arrestin-EA

Agonist	EC_{50}	pEC_{50} ± SEM	E_{max} ± SEM
SLIGKV	N. R	N. R	N. R
SLIGRL	N. R	N. R	N. R
GB110	N. R	N. R	N. R
2f-LIGRLO	N. R	N. R	N. R